Final Technical Report
On

Fundamental Limits to Compact, Expendable Pulsed Power and Microwave Sources

Air Force Office of Scientific Research
Grant No. F49620-97-1-0476

Submitted September 14, 2000

M. Kristiansen, Director
Pulsed Power Laboratory
Department of Electrical Engineering
Texas Tech University
Lubbock, Texas 79409-3102

Attn: Robert Barker
AFOSR/NE
801 North Randolph Street
Room 732
Arlington, VA, 22203-1977

REPORT DOCUMENTATION PAGE

AFRL-SR-BL-TR-00-

0539

1. AGENCY USE ONLY (Leave blank)	2. REPORT DATE	3. REPORT TYPE AND DATES COVERED
	14 Sept., 2000	Final, 15 June 1997 - 14 June 00

4. TITLE AND SUBTITLE

Fundamental Limits to Compact, Expendable Pulsed Power And Microwave Sources

5. FUNDING NUMBERS

FQ8671-9701337 (start)
FQ8671-0000337 (end)

6. AUTHOR(S)

M. Kristiansen, J. Dickens, and S. Shkuratov

7. PERFORMING ORGANIZATION NAME(S) AND ADDRESS(ES)

Pulsed Power Laboratory
Dept. of Electrical Engineering
Texas Tech University
Lubbock, TX 79409-3102

8. PERFORMING ORGANIZATION REPORT NUMBER

AFOSR NWV - 4

9. SPONSORING / MONITORING AGENCY NAME(S) AND ADDRESS(ES)

Dr. Robert J. Barker
AFOSR/NE
801 N. Randolph Street, Room 732
Arlington, VA 22203-1977

10. SPONSORING / MONITORING AGENCY REPORT NUMBER

11. SUPPLEMENTARY NOTES

12a. DISTRIBUTION / AVAILABILITY STATEMENT

Approved for public release;
distribution unlimited

12b. DISTRIBUTION CODE

13. ABSTRACT ***(Maximum 200 Words)***

This final report covers activities conducted by Texas Tech University from June 15, 1997 to June 14, 2000. We are investigating the fundamental basic materials limitations to the design of compact, expendable (i.e. one-time use), pulsed power and microwave sources which can be munitions launched, air dropped, towed, etc. These devices will ultimately be driven by explosives but the initial laboratory work was done with electrically driven flyer plates and light gas guns. The main devices of interest include piezoelectric generators, ferromagnetic generators, cylindrical implosion flux compression generators, and helical flux compression generators. Some additional research was focused on the one-time evacuation of e-beam chambers using chemical reactions. The overall goal of the research was to obtain a basic physical understanding of these generators and to establish the fundamental materials limits to their function, taking advantage of thermal and kinetic inertia, one-time dielectric stresses, etc. The longer term, practical goal is to obtain engineering guidelines for developing order of magnitude smaller devices than are possible for present-day, long life, high reliability generators.

14. SUBJECT TERMS Expendable Microwave Sources, Kinetic-Electric Energy Conversion, Light Gas Guns and Explosives

15. NUMBER OF PAGES 49

16. PRICE CODE

17. SECURITY CLASSIFICATION OF REPORT	18. SECURITY CLASSIFICATION OF THIS PAGE	19. SECURITY CLASSIFICATION OF ABSTRACT	20. LIMITATION OF ABSTRACT
Unclassified	Unclassified	Unclassified	

TABLE OF CONTENTS

INTRODUCTION

This New World Vistas Program on Fundamental Limits to Compact, Expendable Pulsed Power and Microwave Sources has involved 3 faculty members, 1 postdoctoral fellows, and one graduate student. The personnel involved are:

	Phone	Fax	E-Mail
M. Kristiansen	806/742-2224	806/742-1281	krisk@coe.ttu.edu
J. Dickens	806/742-1254	806/742-1281	jdickens@coe.ttu.edu
S. Shkuratov	806/742-3974	806/742-1281	sshkuratov@ppl.ee.ttu.edu
J. Kim	806/742-3507	806/742-1281	
B. McCuistian (now at LANL)	505/667-7022	505/667-7684	trentmc@plasmasys.lanl.gov

The main activities under this program are as follows:

a. Fundamental limits to explosively driven, compact pulsed power generators.
b. Conversion of kinetic to electric energy utilizing piezoelectric, ferromagnetic, and magneto-strictive effects.
c. Determination of ultimate performance limits of electrical components (capacitors, resistors, etc.) for short life use.
d. Possible uses of chemical techniques to evacuate high power microwave diode-systems and thus make large pumping systems unnecessary.

EXECUTIVE SUMMARY

This New World Vistas program on Fundamental Limits to Compact, Expendable Pulsed power and Microwave Sources emphasizes research on one-time use components. This is quite different in philosophy and approach from the "classical" systems where lifetime and long term reliability is at a premium. In the program described here, the effort is on stressing components and systems to the maximum for a short period (maybe less than 1 μs) or for a short burst (maybe 5 pulses) at high repetition rate. This implies for instance that cooling and heat sinking is of limited or no use. Adiabatic design and reliance on thermal and kinetic inertia are, therefore, part of the design philosophy. It has been determined that standard circuit components, such as common carbon resistors, can be operated at nearly six orders of magnitude higher power than their rated values for several tens of microseconds without major changes in their rated values.

It also appears that the energy storage density of capacitors may be increased by a factor of ten for one time use. We planned to work with Maxwell/Physics International Co. on this particular issue. They have agreed to provide us with test samples for this work but their samples never arrived. An automated component test facility was designed and built and components on-hand were tested.

The initial work has been devoted to shock induced pulsed power by kinetic impact on ferromagnetic and piezoelectric materials and by converting the kinetic energy of accelerated magnetic materials to electric signals. In this work the kinetic energy was produced by a conventional light gas gun and later used actual explosives to generate shock waves and accelerate samples. We have developed various scaling laws (experimentally and theoretically) that are being tested (verified) at high kinetic energies which can only be conveniently obtained by explosive methods. A new explosive facility is ready in the East Building of the Pulsed Power Laboratory and the explosives tests will continue at this site.

We have also conducted a small test of a possible method to evacuate microwave sources by chemical methods which may make it unnecessary to use large, heavy vacuum pumping equipment. This has met with some success and will be continued in cooperation with a colleague who has moved to Mercer University in Macon, Georgia. We are lending him some equipment but plan not to use any further contract monies for this effort except for possible publication charges.

In this NWV work, it is important to understand that although long term, conventional reliability is not important, it is still important that the devices work <u>once</u> with high reliability. This implies a totally different mindset and testing philosophy and also a detailed understanding of the basic physics issues behind the failure mechanisms.

RESEARCH TASKS

A summary of our methodology for six research tasks and the results are given for the period, 15 June 1997 to 14 June 2000.

I. EXPLOSIVELY DRIVEN SHOCK WAVE FERROMAGNETIC GENERATORS

Design of shock wave ferromagnetic generators

We use two different approaches for designing compact reliable explosively driven pulsed power systems. The first approach is based on fundamental effects of solid-state physics and effects associated with the action of shock waves on a solid. The function of a single-use system for pulse generation is the conversion of the ferromagnetic or ferroelectric energy into a single high-power pulse of electrical energy. Another approach for designing compact efficient pulsed power systems is the conversion the kinetic energy of ferromagnetic projectiles into the energy of electric pulses.

We performed a series of experiments of generation of high current pulses using explosively driven shock wave ferromagnetic generators. A shock wave ferromagnetic generator is shown schematically in Fig. 1. In this series of experiments we used an open ferromagnetic circuits design. An open ferromagnetic circuit is a ferromagnetic system having unclosed N-S poles and where the magnetic flux closes through a nonferromagnetic medium or through the space surrounding the two magnetic poles. We performed shock wave experiments with two different types of ferromagnetic active elements: NdFeB cylinders D = 2.5 cm, L = 1.9 cm and $BaFe_2O_3$ cylinders D = 2.2 cm, L = 2.5 cm.

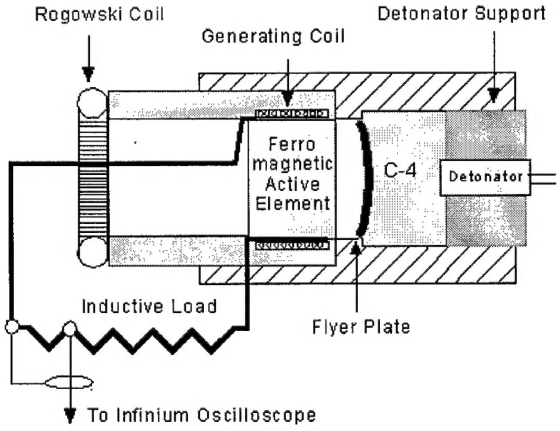

Figure 1. Schematic of the shock wave ferromagnetic generator.

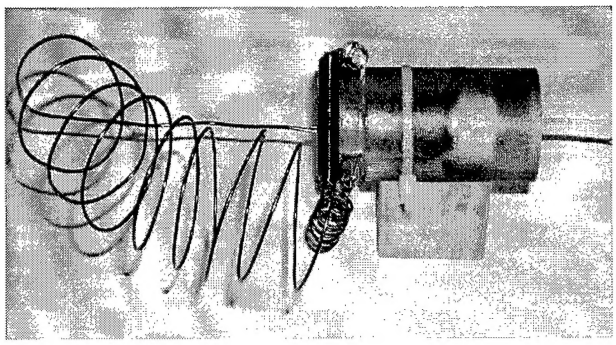

Figure 2. The shock wave ferromagnetic generator in the charged state. The active element is an NdFeB cylinder D = 2.5 cm, L = 1.9 cm. Mass of C-4 is 15 g.

The general appearance of the shock wave ferromagnetic generator in the charged state is shown in Fig. 2. In all explosive shock wave experiments type C-4 high explosive was used. In this set of shock wave experiments we used flyer plates. We had axial detonation of the high explosive. The shapes of the flyer plates were precisely calculated so that a plane shock wave was generated in the ferromagnetic active element.

Figure 3 presents an electrical circuit of the shock wave ferromagnetic generator. All generators in this series of experiments operated in the current mode (a low-resistance load). For the NdFeB active elements (D = 2.5 cm, L = 1.9 cm) the pulse-generating coils had eight turns which were wound with round copper wire in one layer. For the $BaFe_2O_3$ active elements (D = 2.2 cm, L = 2.5 cm) the pulse-generating coils had eleven turns which were wound with round copper wire in one layer. All generators were furnished with calibrated Rogowski coils and integrators to measure directly the current flowing in the load circuit. The voltage was picked from a portion (2.5 mΩ/0.9 μH) of the load. We used 50 Ω inputs of the Infinium oscilloscopes to decrease the noise level. In a few tests we used a 5 mΩ load. In the main body of the shock wave experiments, the load parameters were comparable to the parameters of the primary winding of the flux compressor generator used in our MURI (Multi University Research Initiative) experiments. The resistance of the load was 19 mΩ and its inductance was 6.7 μH.

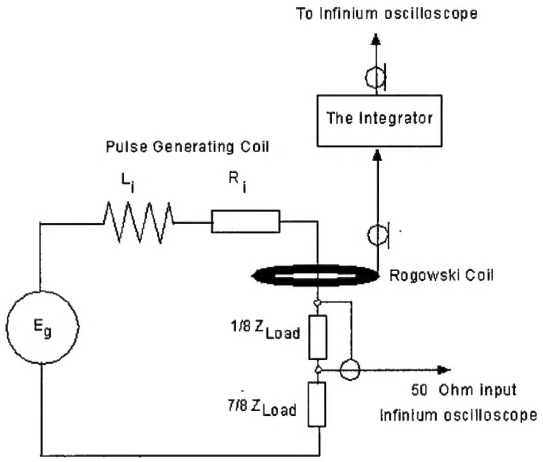

Figure 3. Electrical circuit of the shock wave ferromagnetic generator.

Explosive operation of the shock wave ferromagnetic generator

The generation of high current and high voltage pulses in the shock wave ferromagnetic generator is based on the demagnetization of ferromagnetic materials by a mechanical shock. A shock wave randomly orients the magnetic moments. Randomizing magnetic moments leads to a flux change in the magnetic core and induces voltage in the winding wound on the core. The operation of the shock wave ferromagnetic generator is to reduce or completely destroy the remnant magnetization by a shock wave from a high explosive.

Figure 4 presents a series of photographs of the generator taken during the operation of the explosive charge. The active element was an NdFeB cylinder (D = 2.5 cm, L = 1.9 cm). The C-4 mass was 15 g. The shot-to-shot interval was 4 μs. The high explosive and the flyer plate are pictured at the right-hand. The ferromagnetic active element is at the left-hand. It can clearly be seen that the destruction of the generator's body starts at 16 μs after detonator ignition.

Figure 5 shows the shock wave generator after an explosive test. Figure 6 presents photos of the flyer plate, taken before and after an experiment. It can clearly be seen that the central portion of the flyer plate is not separated from the rest of the plate during the acceleration. Comparing photos of the flyer plates, taken before and after testing, we conclude that a plane shock wave is generated in the ferromagnetic active element.

The current pulse waveform produced by the shock wave generator is given in Fig. 7. The current amplitude is 470 A (5 mΩ load). The current pulse waveform is almost triangular. The FWHM of the pulse is about 25 μs. The rise time is about 6 μs. The voltage pulse waveform is given in Fig. 8. The appearance of the voltage pulse is due to the reaction of the inductive load to the rising current flowing in the load circuit. The duration of the voltage pulses is about 6 μs. The pulse waveform has a multi-peak structure.

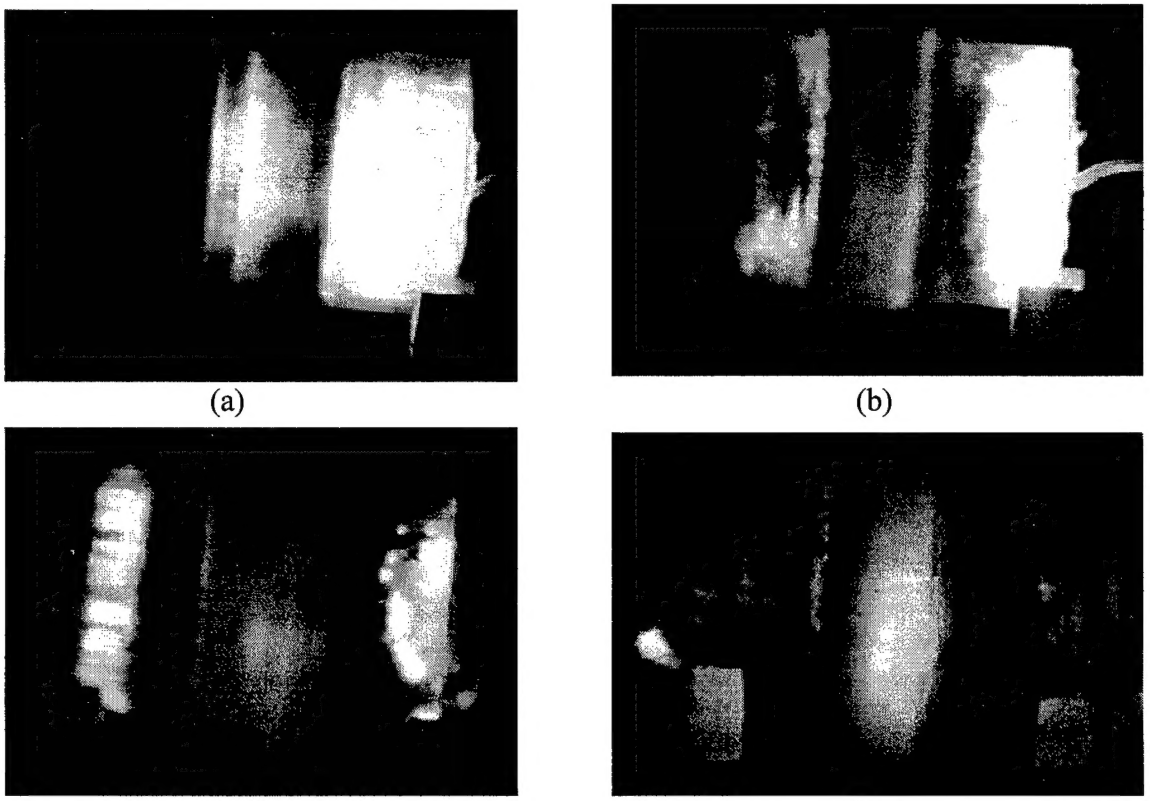

Figure 4. Explosive operation of the shock wave ferromagnetic generator. Shot-to-shot interval is 4 μs. Shown left to right.

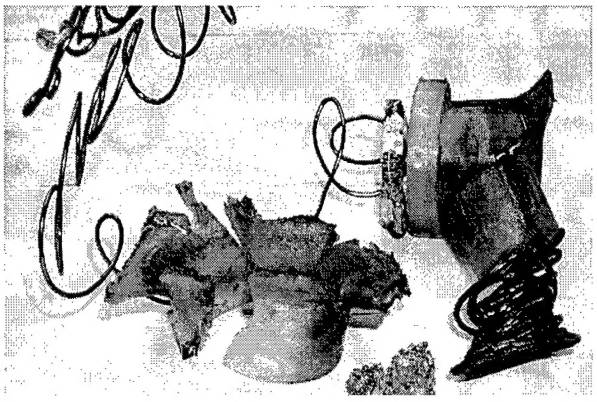

Figure 5. The generator after an explosive test.

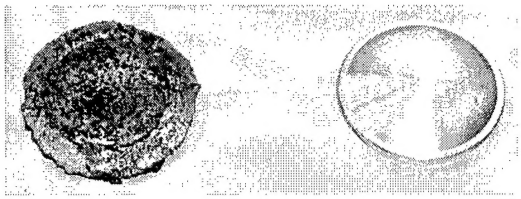

Figure 6. The flyer plate before (right) and after (left) an explosive test.

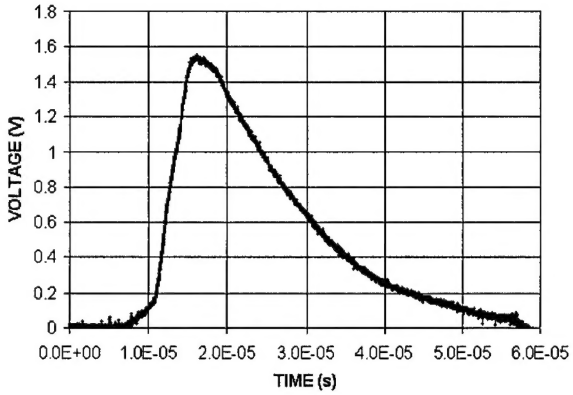

Figure 7. Explosive operation of the shock wave ferromagnetic generator. Waveform of the current pulse (signal from a Rogowski coil). The active element is an NdFeB cylinder (D = 2.5 cm, L = 1.9 cm). The load is 5 mΩ/1.6 μH. 0.29 A/mV.

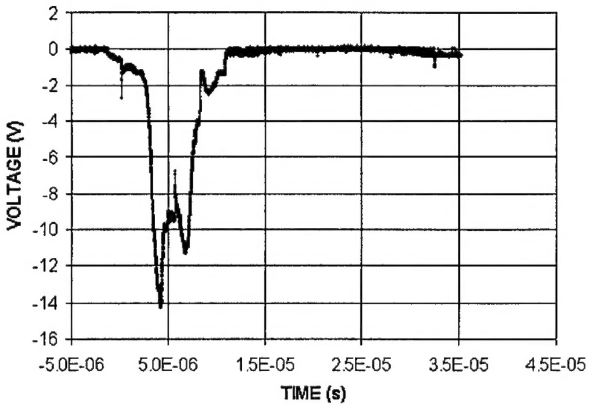

Figure 8. Waveform of the voltage pulse (signal from a portion (2.5 mΩ) of the load). The active element is an NdFeB cylinder (D = 2.5 cm, L = 1.9 cm). The load is 5 mΩ/1.6 μH. Attenuation is 10 dB.

Figure 9 presents the current waveform for the generator with the same active element with a 19 mΩ load. The current waveform has no significant distinctive features from the current waveform across 5 mΩ load. The only difference is the lower current amplitude of 250 A.

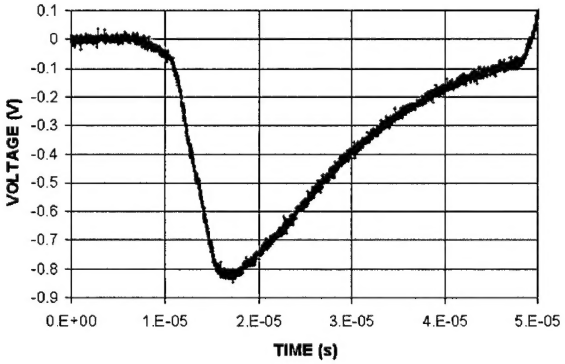

Figure 9. Explosive operation of the shock wave ferromagnetic generator. Waveform of the current pulse (signal from a Rogowski coil). The active element is an NdFeB cylinder (D = 2.5 cm, L = 1.9 cm). The load is 19 mΩ/6.7 μH. 0.3 A/mV.

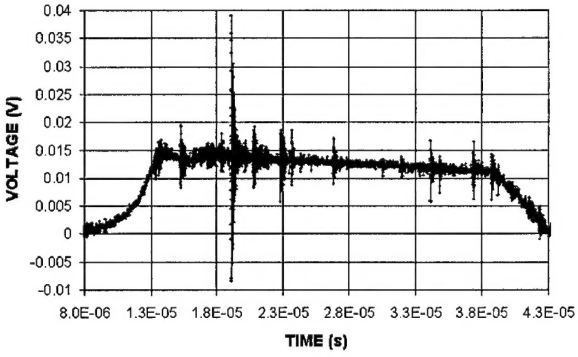

Figure 10. Waveform of the current pulse (signal from a Rogowski coil). The active element is a $BaFe_2O_3$ cylinder (D = 2.2 cm, L = 2.5 cm). The load is 19 mΩ/6.7 μH. 3.1 A/mV.

We carried out a series of explosive tests with shock wave generators having hard ferrite active elements. The design of the generators in these experiments was identical to the design of the generator with NdFeB cylinders. The current pulse waveform of the generator is given in Fig. 10. The current amplitude is about 50 A and the pulse FWHM is about 25 μs. If we suppose that the pulse was produced on one pass of the shock wave generated in the ferrite body, we obtain that the velocity of the shock wave was about 1 km/s.

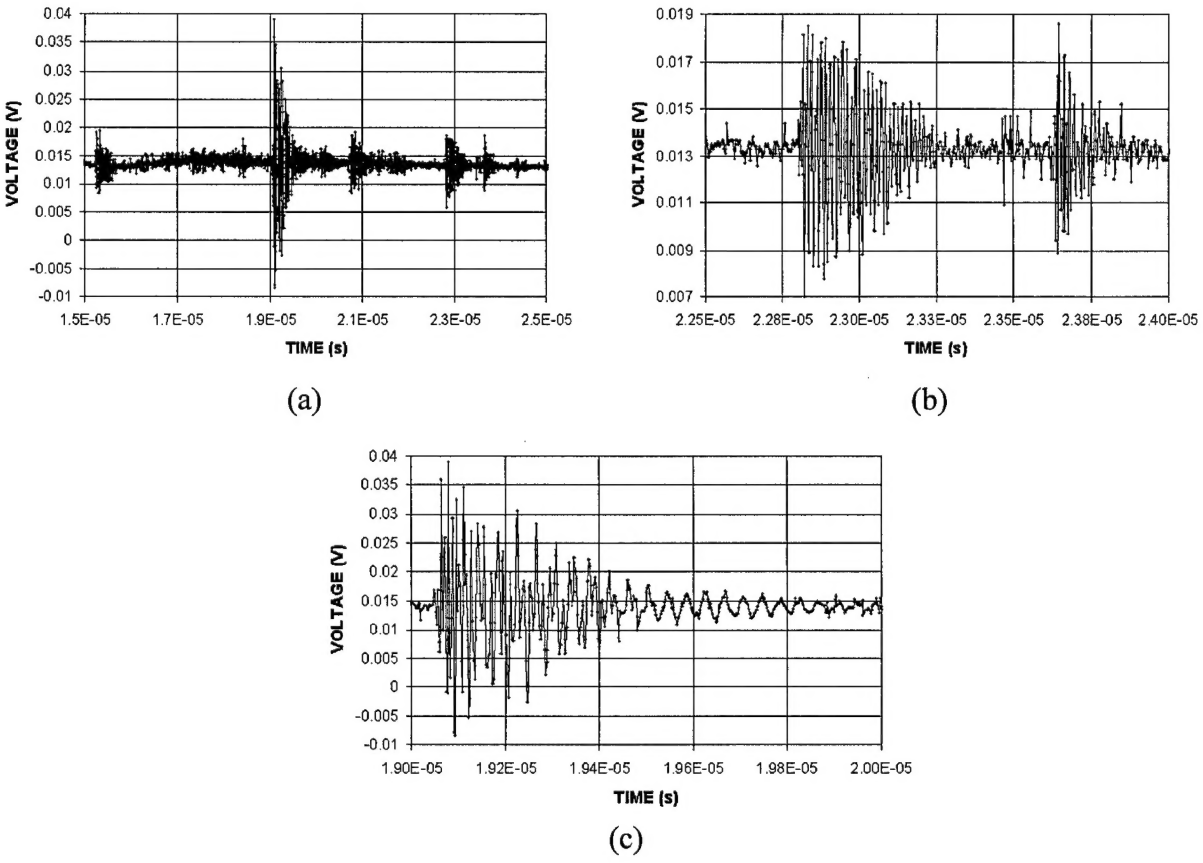

Figure 11. Portion of the waveform of the current pulse (presented in Fig. 10) in a magnified time scale.

Two features can be noted in the behavior of the current pulse of $BaFe_2O_3$ active element. First, unlike experiments with NdFeB cylinders (Figs. 7 and 9), the current pulse waveform in these tests was close to rectangular. Second, the current pulse contains high frequency oscillations. Figure 11 presents portions of the current waveform in a magnified time scale. There are several bunches of high frequency oscillations. The time interval between bunches is 2-4 μs. The width of every bunch is 200-400 ns. The frequency of the oscillations is about 100 MHz. Peak-to-peak current reaches 100 A. It is possible that the high frequency signal was changed by the Rogowski coil integrator. Possibly the reason for differences in the current pulse behavior of hard ferrite tests and NdFeB tests is that unlike NdFeB the ferrite cylinder is a high resistance, non-linear material.The voltage pulse waveform of a $BaFe_2O_3$ active element is given

in Fig. 12. Here two separate voltage pulses can clearly be distinguished. The appearance of two voltage pulses is the reaction of the inductive load to the rising and the falling current flowing in the load circuit. The time interval between pulses is 25 μs.

Magnetic Flux in an Open Circuit

The amplitude of the pulse produced in the pulse-generating coil depends on the rate of variation of the magnetic flux inside the coil and the parameters of the coil. Manufacturers of the magnetic materials supplied information about the properties of ferromagnetic materials in a closed circuit. A closed ferromagnetic circuit is a ferromagnetic system having closed poles and in which the magnetic flux circulates inside the circuit with little flux in the surrounding nonferromagnetic space. Characteristics for NdFeB and $BaFe_2O_3$ in a closed circuit are given in Table 1. In this series of experiments we used open ferromagnetic circuit designs. We performed a simulation of the magnetic flux density **B** and the magnetic intensity **H** of NdFeB and $BaFe_2O_3$ in an open circuit using the Maxwell 3D code.

Table 1. Characteristics of NdFeB and $BaFe_2O_3$ in a closed ferromagnetic circuit.

Material	$\mathbf{B_r}$ (T)	$\mathbf{H_c}$ (A/m)	$\mathbf{H_{ci}}$ (A/m)	$\mathbf{BH_{max}}$ (T·A/m)	**Max. Op. Temp.** (C)
NdFeB (Nd35)	1.23	$9x10^5$	$1.1x10^6$	$2.55x10^5$	150
$BaFe_2O_3$ (Ceramic 5)	0.395	$1.9x10^5$	$1.95x10^5$	$2.86x10^4$	300

$\mathbf{B_r}$ is the residual flux density; $\mathbf{H_c}$ is the coercive force; $\mathbf{H_{ci}}$ is the intrinsic coercive force (the point at which the hysteresis curve crosses the **H** axis); $\mathbf{BH_{max}}$ is the maximum energy product and **Max. Oper. Temp.** is the maximum operating temperature of the magnet.

Figure 13 presents a schematic diagram of the ferromagnetic active element with the winding for magnetic field and eddy currents simulations. Figure 14 presents the magnetic flux density inside and outside the NdFeB cylinder having a diameter of 2.5 cm and length of 1.9 cm.

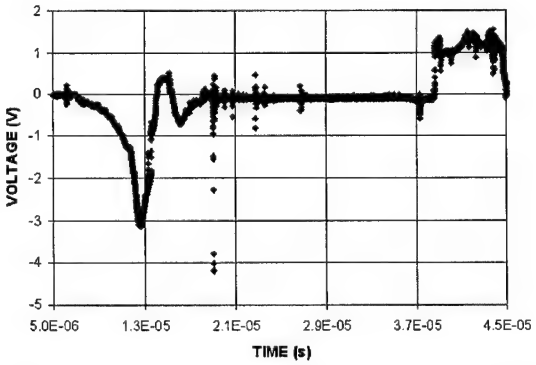

Figure 12. Waveform of the voltage pulse (signal from a portion (2.5 mΩ) of the load). The active element is a $BaFe_2O_3$ cylinder (D = 2.2 cm, L = 2.5 cm). Load is 19 mΩ/6.7 μH.

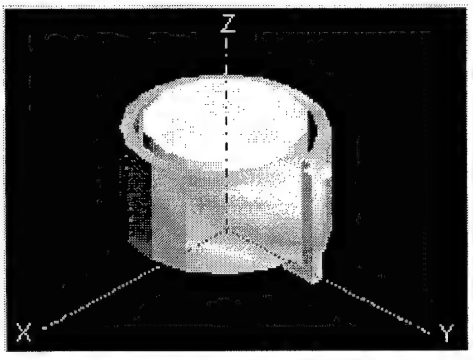

Figure 13. Schematic diagram for magnetic field and eddy current simulations. Magnetic field is orientated along Z axis.

As it follows from the simulation results, the flux density outside the cylinder (flux in an open circuit) is two or three times lower than that inside the cylinder (flux in a closed circuit). The magnetic flux near the cylinder strongly depends on distance and on the position along the cylinder body. The flux near the top and the bottom is about two times higher than the flux near the middle of the cylinder. At a distance of more than 5-8 mm from the cylinder the magnetic flux varies slowly and the difference in fluxes at different positions along the cylinder is not so large.

Figure 15 presents the magnetic flux density inside and outside the NdFeB cylinder having a diameter of 2.5 cm and length of 3.8 cm. Comparing the simulation results for cylinders of length 1.9 cm (Fig. 14) and 3.8 cm, one can make a conclusion that an increase in magnetic cylinder length leads to a decrease in magnetic flux near the middle of the cylinder. Relatively short ferromagentic active elements, large in diameter, possess higher energy for pulsed power generation. Figure 16 presents magnetic flux density inside and outside the $BaFe_2O_3$ (hard ferrite) cylinder having D = 2.2 cm and length of 2.5 cm. The magnetic flux outside the core does not exceed 0.15 T.

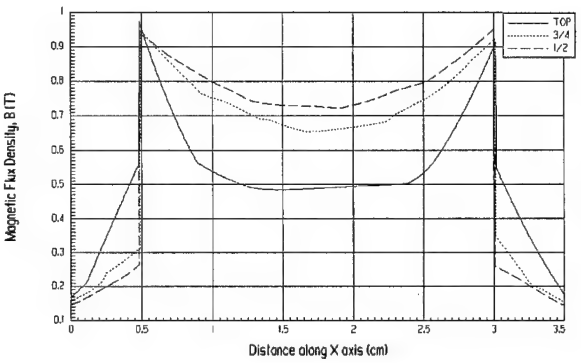

Figure 14. Magnetic flux density inside and outside an NdFeB cylinder (D = 2.5 cm, L = 1.9 cm). Solid line is the distribution at the top of the cylinder. Dotted line is the distribution at the 1.4 cm height (3/4 of cylinder's height). Dashed line is the distribution at the 0.95 cm height (1/2 of cylinder's height).

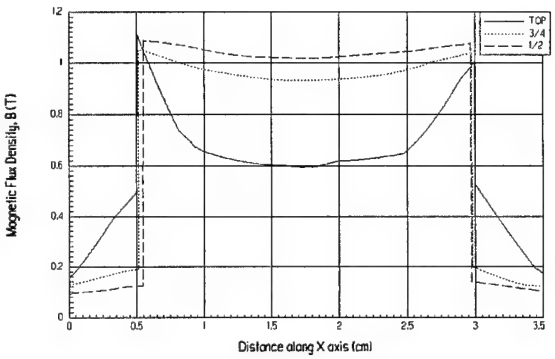

Figure 15. Magnetic flux density inside and outside an NdFeB cylinder (D = 2.5 cm, L = 3.8 cm). Solid line is the distribution at the top of the cylinder. Dotted line is the distribution at the 2.8 cm height (3/4 of cylinder's height). Dashed line is the distribution at the 1.9 cm height (1/2 of cylinder's height).

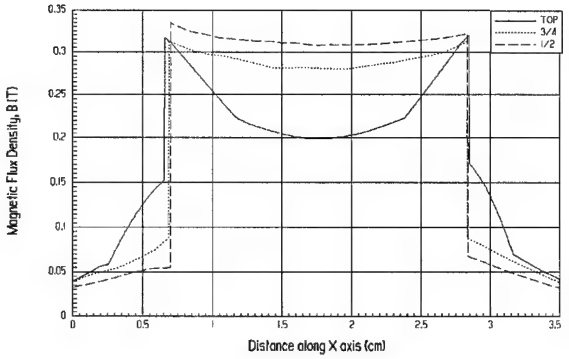

Figure 16. Magnetic flux density inside and outside a $BaFe_2O_3$ cylinder (D = 2.2 cm, L = 2.5 cm). Solid line is the distribution at the top of the cylinder. Dotted line is the distribution at the 1.9 cm height (3/4 of cylinder's height). Dashed line is the distribution at the 1.25 cm height (1/2 of cylinder's height).

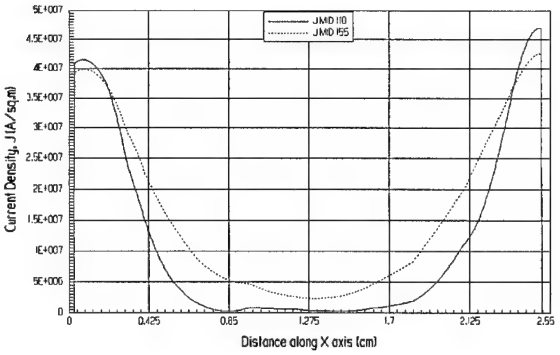

Figure 17. Distribution of the eddy curent density along the radius (X axis) in the body of an NdFeB cylinder (D = 2.5 cm, L = 1.9 cm). The change in the magnetic flux: 0.2 T during 6 μs. Solid line is the eddy current density at 3 μs after current starting point. The current is 669 A at this moment. Dotted line is the eddy current density at 6 μs after current starting point. The current is 950 A at that moment.

Eddy Currents

When a shock wave propagates in a solid magnetic cylinder, there occurs disorientation of the magnetic moments resulting in a decrease or complete disappearance of residual magnetization. As this takes place, some accompanying processes occur. The magnetic flux in the cylinder, rapidly varying under the action of the shock wave, induces eddy currents which in turn induce a magnetic field of strength **H** directed to keep the magnetic flux at its initial level. In the coil wound on the cylinder a current is generated which induces a magnetic field directed, like the field created by eddy currents, to keep the magnetic flux at its initial level. The operating point on the magnetization curve moves to the right. We performed a simulation of eddy currents in the core using the Maxwell 3D code. Figure 17 presents the eddy current density distribution in the NdFeB cylinder.

As it follows from the simulation results, eddy current amplitude in the NdFeB body reaches a significant value, 950 A. The generation of eddy currents in the magnetic cylinder reduces the efficiency of the generation of a current pulse in the pulse-generating coil. The amplitude of the pulse generated in the coil is directly proportional to the resulting change in the magnetic flux density in the active element $\Delta\mathbf{B} = \mathbf{B_r} - \mathbf{B_0}$, where $\mathbf{B_r}$ is the initial magnetic flux density in the core and $\mathbf{B_0}$ is the flux density remaining in the core. The resulting change in magnetic flux density in the active element is responsible for the generation of the current pulse. To estimate the resulting change in magnetic flux density in the ferromagnetic cylinder responsible for the generation of the current pulse, we have performed a simulation of the processes occurring in the ferromagnetic core with the use of the Maxwell Simulator and experimental data of explosive tests. The estimation of the resulting change in magnetic flux in a pulse-generating system with the NdFeB active elements gives $\Delta\mathbf{B}$ = 0.05-0.1 T. This is less than 20% of the magnetic flux of the NdFeB cylinders in an open circuit.

To suppress eddy currents in the ferromagnetic active element and to increase the efficiency of the shock wave ferromagnetic generator it is necessary to redesign the pulse-generating unit, to split it into separate parts insulated from each other. We designed an active element which consists of a number of thin insulated NdFeB plates. We simulated the magnetic flux density and eddy currents in such an active element by the Maxwell 3D code.

Figure 18 presents distribution of the eddy current density along the radius (X axis) in the combined active element: the NdFeB cylinder, having diameter 2.5 cm and length 1.9 cm, consists of 52 thin insulated Nd35 plates (0.4 mm plate thickness and 0.1 mm plate-to-plate distance). The magnetic flux change is 0.2 T during 6 μs. The eddy current peak amplitude is just 0.33 A. As it follows from simulation results there is practically no eddy currents in the combined active element.

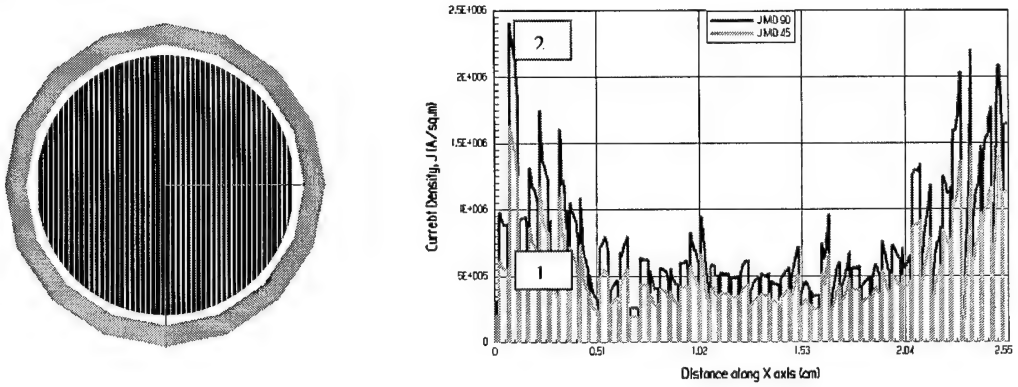

(a) (b)

Figure 18. Eddy current simulation. (a) - top view of combined active element: NdFeB cylinder having diameter D = 2.5 cm, length L = 1.9 cm consists of 52 insulated plates (0.4 mm thickness and 0.1 mm plate-to-plate distance). (b) - distribution of eddy current density along the radius. The change in magnetic flux: 0.2 T during 6 μs. Curve 1 (gray) is the eddy current density distribution at 3 μs after current starting point. The current is 0.29 A at this moment. Curve 1 (black) is the eddy current density distribution at 6 μs after current starting point. The current is 0.33 A at this moment.

Figures 19 presents the magnetic flux density inside and outside the NdFeB combined active element, across the plates. Comparing the simulation results for the whole NdFeB cylinder of D = 2.5 cm and L = 1.9 cm (see Fig. 14) and the combined active element, one can conclude that there is no significant magnetic flux loss in the combined active element.

Figures 20 presents distribution of the eddy current density along the radius in the NdFeB cylinder (D = 2.5 cm, L = 1.9 cm) having 24 radial cuts (5.5 mm depth, 0.5 mm thickness). The eddy currents peak amplitude is 421 A. The current flows in the central part of the cylinder. There practically no current at the cylinder edge.

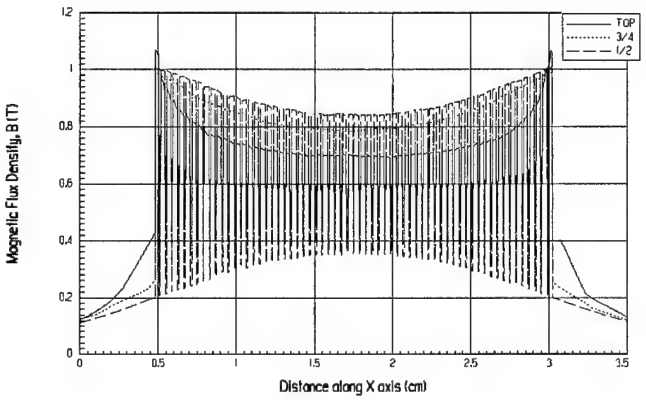

Figure 19. Magnetic flux simulation. Magnetic flux density inside and outside combined active element having 52 NdFeB insulated plates attached to each other. Thickness of one plate is 0.4 mm. Plate-to-plate distance is 0.1 mm. Diameter of the active element as a whole is 2.5 cm and length 1.9 cm. Solid line is the distribution at the top of combined active element across the NdFeB plates. Dotted line is the distribution at the 1.4 cm height (3/4 of cylinder's height). Dashed line is the distribution at the 0.95 cm height (1/2 of cylinder's height).

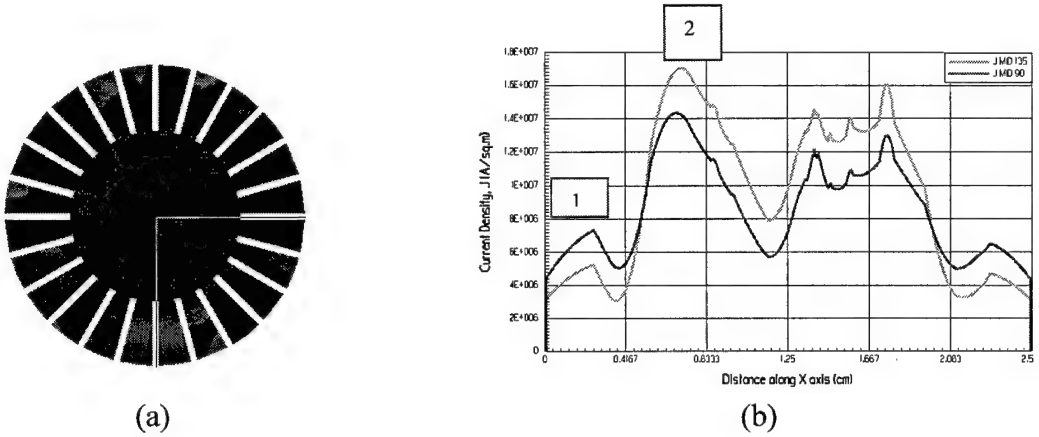

(a) (b)

Figure 20. Eddy current simulation. (a) - top view of the active element: NdFeB cylinder having (D = 2.5 cm, L = 1.9 cm) having 24 cuts (5.5 mm depth, 0.5 mm thickness). (b) - distribution of eddy current density along the radius. The change in magnetic flux: 0.2 T during 6 μs. Curve 1 (black) is the eddy current density distribution at 3 μs after current starting point. The current is 337 A at this moment. Curve 2 (gray) is the eddy current density distribution at 6 μs after current starting point. The current is 421 A at this moment.

Using the results of simulation we have designed and built a shock wave ferromagnetic generator with a combined active element. Figure 21 presents the design of an explosive OFC generator with an NdFeB combined active element.

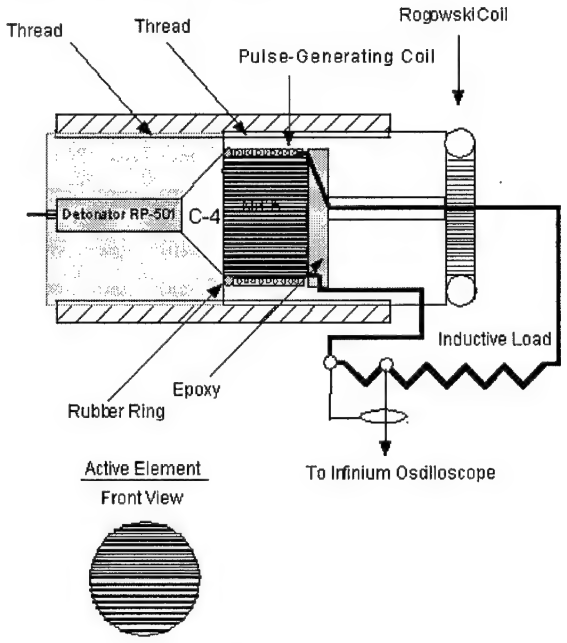

Figure 21. Schematic of the shock wave ferromagnetic generator with an NdFeB combined active element.

We designed two different models of combined active elements. Five devices are prepared for explosive experiments which are planned in September 2000 at the new explosive facilities of the Pulsed Power Laboratory. The explosive tank for experiments with small amounts of high explosive (10-30 g) is shown in Fig. 22.

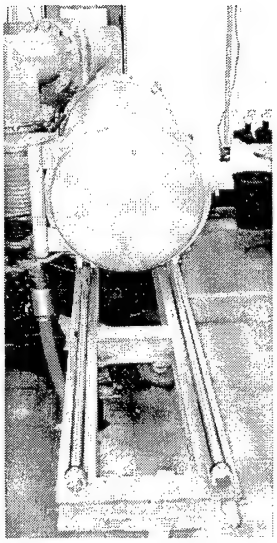

Figure 22. Explosive tank for experiments with small amounts of high explosives. Diameter is 68 cm. Length is 155 cm. Stainless steel wall thickness is 11.1 mm.

Electrical Circuit Simulation

In order to understand the multi-peak structure of the voltage pulse across the load in experiments with NdFeB cylinders (see Fig. 8) we performed simulation of electrical circuit of the shock wave ferromagnetic generator. The equivalent circuit of the generator is presented in Fig. 23. R_{gc} and L_{gc} are the resistance and inductance of the pulse-generating coil. R_{load1} and L_{load1} are the resistance and inductance of the first part of the load (16.5 mΩ). R_{load2} and L_{load2} are the resistance and inductance of the second part of the load (2.5 mΩ). Voltage Probe 1 gives the waveform of the voltage pulse across the whole load. Voltage Probe 2 gives the waveform of the voltage pulse across the second part of the load as we measured in the experiments. A current probe placed between the pulse generating coil and the load is exactly like the Rogowski coil that was placed in the experimental setup.

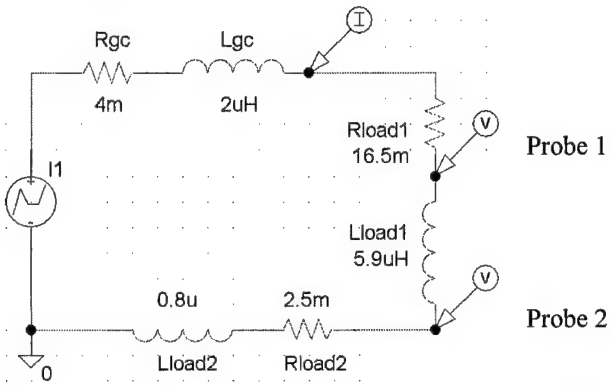

Figure 23. Equivalent circuit of the shock wave ferromagnetic generator.

Figure 24 shows the rise time of the actual current pulse produced by the shock wave generator with a NdFeB active element in a magnified time scale. The current pulse amplitude is 230 A. It can clearly be seen that these are two different slopes of current rise. The presence of two slopes in the current rise is possibly the result of specific features of the initiating shock wave in the body of the NdFeB cylinder. Figure 25 shows the actual voltage pulse across a part of the load (2.5 mΩ) in a magnified time scale.

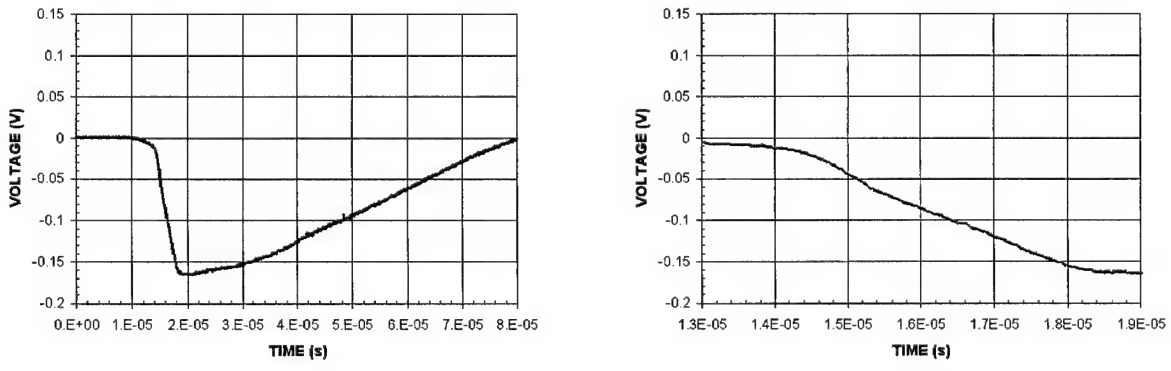

(a) (b)

Figure 24. (a) - waveform of the current pulse (signal from a Rogowski coil). The active element is an NdFeB cylinder (D = 2.5 cm, L = 1.9 cm). The load is 19 mΩ/6.7 μH. 154 A/V. (b) - rise time in a magnified time scale.

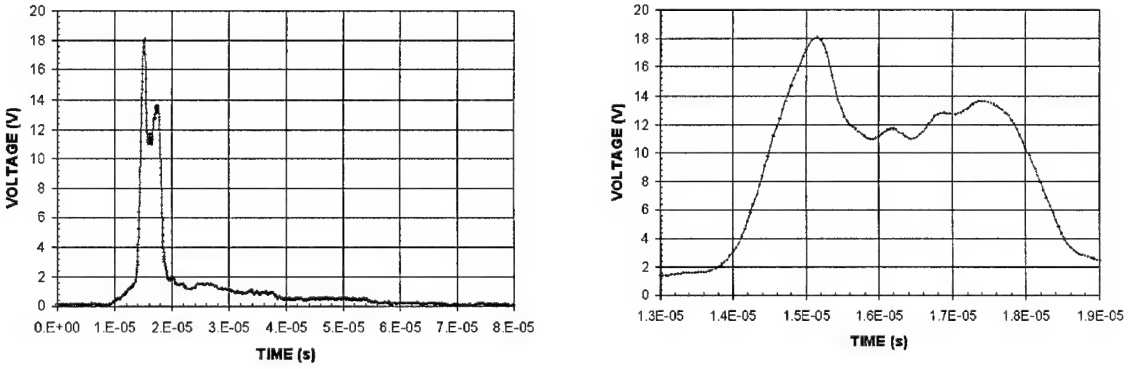

(a) (b)

Figure 25. (a) - waveform of the voltage pulse (signal from a portion of the load (2.5 mΩ)). The active element is an NdFeB cylinder (D = 2.5 cm, L = 1.9 cm). The load is 19 mΩ/6.7 μH. (b) - part of the signal in a magnified time scale. Attenuation 10 dB.

Figures 26 shows results of a simulation of the signal in the load circuit of the generator using the PSpice code. The shape of the current pulse was close to the experimental one. Both the voltage pulse across the whole load as well as the voltage pulse across a part (2.5 mΩ/0.9 μH) of the load demonstrates a two-peak structure. The amplitude of the voltage is directly proportional to the value of the load, 480 V across the whole load (19 mΩ/6.7 μH) and 55 V across a part (2.5 mΩ/0.9 μH) of the load. In comparing the experimental waveform of the voltage (Fig. 25) and the calculated waveform (Fig. 26) one can see qualitative agreement.

Summary

A design was developed for compact and expendable explosively driven shock wave ferromagnetic generators. Experimentally, we showed that it is possible to generate a high current pulses in open ferromagnetic circuit generators based on shock wave demagnetization of hard rare-earth intermetallic compounds. Simulations of magnetic flux in an open circuit using Maxwell 3D code allowed us to determine the optimal shape of ferromagnetic active elements, and thus to give higher energies for pulsed power generation. Simulation of the processes occurring in the ferromagnetic core with the use of the Maxwell Simulator showed that eddy currents are the main reason for energy loss in shock wave ferromagnetic generators. To increase the efficiency of pulsed power generation it is necessary to redesign the pulse-generating unit to suppress eddy currents in the ferromagnetic body. Such experiments are planned at the new explosive facilities of the Pulsed Power Laboratory in September 2000. Particular attention should be given to the effect of the load circuit on the parameters of the generated pulse.

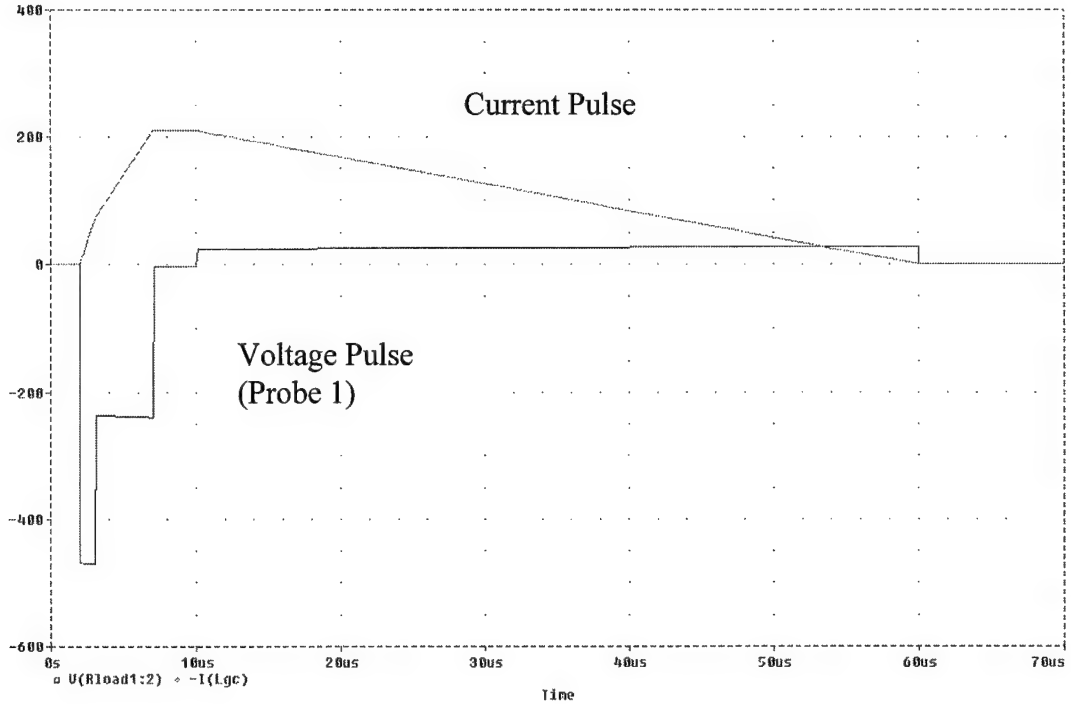

(a)

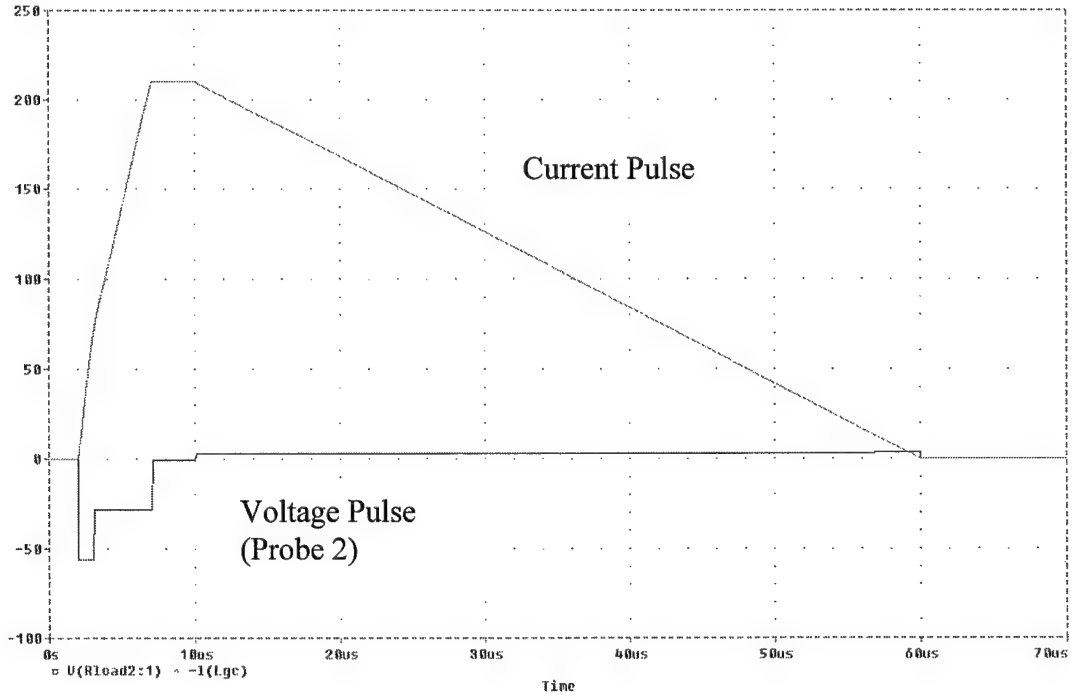

(b)

Figure 26. Electrical circuit simulation. (a) - current pulse waveform (top) and signal from Voltage Probe 1 (bottom). (b) - current pulse waveform (top) and signal from Voltage Probe 2 (bottom).

II. PIEZOELECTRIC PULSE GENERATION

Flyerplate Experiments

An experimental apparatus to launch flyerplates was constructed with the intent of using the impact of these flyerplates to produce a mechanical shockwave in ferroelectric or ferromagnetic materials to produce an electrical pulse. This electromagnetic launcher (EML) consisted of six 200 μF, 10 kV capacitors which could be charged and then discharged, using an ignitron, through a flat inductor on which the flyerplate rested. Copper and aluminum flyerplates of several dimensions were tested and the optimum plate for this EML was found to be an aluminum plate with a diameter of 40 mm and a thickness of 3 mm. Using this plate and a capacitor charge voltage of 4.5kV, the inductor current was about 100 kA and the flyerplate attained a speed of 225 m/s. This speed was too low to produce the desired shockwave.

A computer code was written to simulate the EML and the plate motion. It was found that the flyerplate was initially accelerated to speeds two to three times greater than its final velocity. The initial acceleration was due to the first quarter period of the current in the inductor, however, during the peak current when the rate of change of magnetic field is zero, the motion of the plate in the magnetic field became the dominant force producing mechanism and this slowed the plate. This deceleration was verified experimentally using a high-speed camera to record the position of the plate as it left the surface of the inductor.

To make use of the maximum speed, the target would have to be placed less than one cm from the inductor. With the target so close to the inductor and with such a large rapidly changing magnetic field, electrical measurements on the target would be impossible due to induced voltages. A complete redesign of the inductor and capacitor bank would have been required to get the flyerplate out of the magnetic field before the current in the inductor reached the peak value. The flyerplate approach was dropped.

Rifle Mechanism Experiments

A 30.06 rifle mechanism was installed in a heavy steel tank, which could be sealed and evacuated. This gun accelerated a 7.6 mm diameter, 8.4 gram, copper-clad lead projectile to a speed of 840 m/s. Evacuation of the chamber did not produce a meaningful increase in speed so the experiments were conducted at atmospheric pressure.

Tests of the shock wave produced by this projectile incident on a target were conducted with poled piezoelectric cylinders. The piezoelectric material for the initial tests was chosen because it has been studied and reported on in the literature. Poled cylinders of 35/65 PZT (lead zirconate titanate) 2.54 cm in diameter, and 2.54 cm long were obtained. The remnant polarization of PZT is 30 μC/cc and this is the maximum charge that could be released into a load when the material is subjected to a large amplitude shockwave. The target assembly is shown in Figure 27. This assembly was mounted in the steel tank and struck on the impactor plate by the projectile. The output voltage across a 40 $\pm$ 2 mΩ current viewing resistor was recorded on a digital oscilloscope. Impactor plates of brass and stainless steel and of three thicknesses (25, 19, and 13 mm thick) were used to optimize the shock transferred to the target.

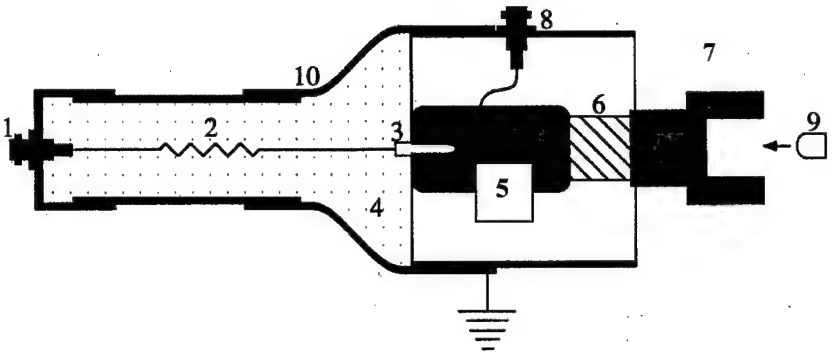

Figure 27. Piezoelectric target transducer. (1) - shorted BNC. (2) - current viewing resistor 40 mΩ. (3) - banana plug. (4) - insulating potting. (5) - 25mm diameter by 50mm long brass backing plate. (6) - 22mm diameter by 23mm long PZT target (- end on impactor plate, + end on backing plate. (7) - impactor plate. (8) - BNC for output signal. (9) - incoming projectile. (10) - copper tubing.

Figure 28 shows the voltage recorded in a typical shot. On this scale this appears to be noise but is actually a series of pulses generated as the PZT target disintegrates into small fragments. Figure 29 shows the structure of the pulses in the time between 15 and 17 μs. Each pulse is a decaying sinusoid with a frequency which is a resonance in the target assembly. Several of the pulses have peaks, which exceed 200 A through the 40 mΩ load. This pattern is characteristic of excessive shock loading of the PZT. A shock of lesser amplitude would produce a more orderly voltage signal but not necessarily more energy in the load.

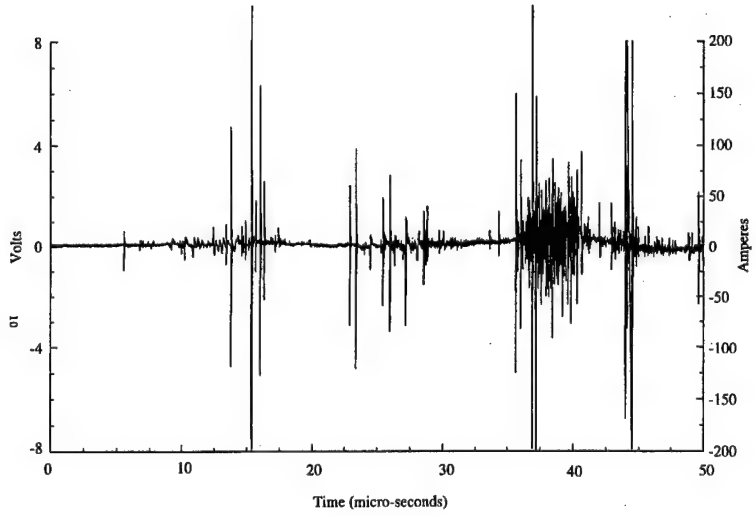

Figure 28. Output voltage and current vs. time (PZT).

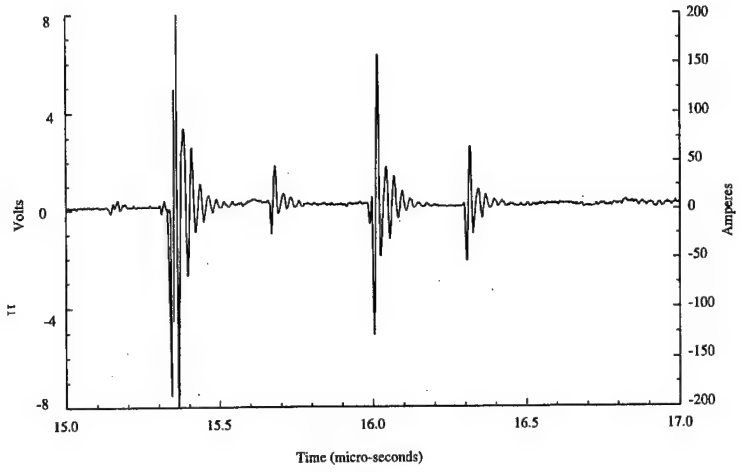

Figure 29. Output voltage and current vs. time (PZT).

The same target assembly was adapted for use with thin films of PVDF (polyvinylidene fluoride). PVDF has a higher remnant polarization than PZT but is difficult to obtain in pinhole free sheets and more difficult to polarize. Figure 30 shows the voltage recorded for a typical shot on a PVDF disk 19 mm in diameter and 0.025 mm thick. This is a decaying sinusoidal pulse showing that the PDVF did not disintegrate but, of course, it was depolarized. The current in this case was only 3.75 A because the volume of the sample was small and only a small amount of charge was available.

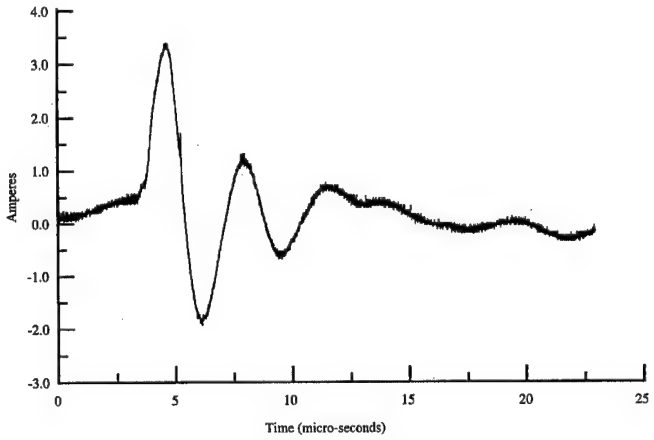

Figure 30. PVDF shock wave waveform.

Explosively Driven Shock Wave Piezoelectric Generators

Using the data received in experiments carried out with explosively driven shock wave ferromagnetic generators and the results of experiments using a rifle mechanism, we have designed and built the first prototype of the compact high-power explosively driven shock wave piezoelectric generator.

We designed three different models of compact explosive piezoelectric generators. Five devices are prepared for explosive experiments that are planned in September 2000. Figure 31 presents a design of an explosive piezoelectric generator.

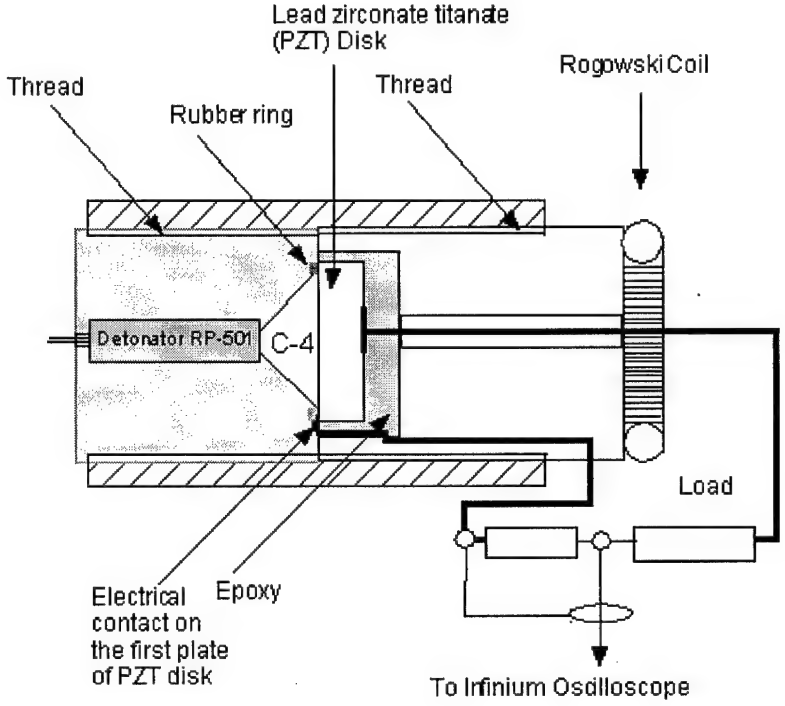

Figure 31. Design of explosively driven shock wave piezoelectrci generator Model 1. Diameter of the device is 5 cm. Length of the device is 12 cm. The active element: Lead Zirconate Titanate (PZT) disk D = 2.5 cm, L = 2.5 mm.

III. MOVING MAGNET SYSTEMS

Gas Gun Kinetic Energy Converter

The experimental study was performed with the use of a light helium gas gun. Schematic diagram of a gas gun kinetic energy converter is presented in Fig.32. The limiting gas pressure in the gas gun reservoir was 1000 psi. Two types of valves were used: an electrically controllable fast acting poppet valve and a rupture disc burst valve. The barrel lengths were 2.44 to 3.5 m. Ferromagnetic projectiles of 1.27 cm and 2.54 cm diameters were used in the experiments. The speed of the magnetic projectile was measured with two independent trigger coil systems installed before and after the generating unit. The gas gun was located in a steel cylindrical chamber having a length of 4.5 m and inner diameter of 0.48 m. A multilayer catch box was used to absorb the high speed ferromagnetic projectile.

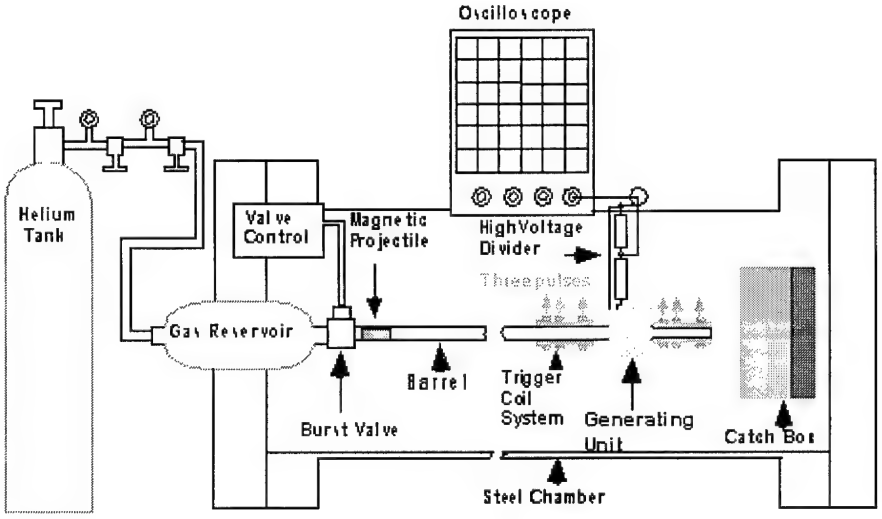

Figure 32. Schematic diagram of gas gun kinetic energy converter.

Open Ferromagnetic Circuit Pulsed Power Generation

The Voltage Mode

Figure 33 illustrates the operation of a pulse generator based on an open ferromagnetic circuit. The motion of the ferromagnetic projectile changes the magnetic flux in the inductance coil and, as a result, an electric pulse is generated across the load.

Figure 34 presents a typical waveform of the high voltage pulses produced by an OFC generator operated in the voltage mode (a high-resistance load) with the 2.5 cm diameter and 3.8 cm length NdFeB projectile moving with a speed of 330 m/s. The peak-to-peak voltage released in a 25 kΩ load is 33 kV. One of the advantages of this concept of pulse generation is that the high voltage pulses produced are highly reproducible and show an extremely low level of noise.

A series of measurements have been performed to investigate the effect of the velocity of the magnetic projectile on the peak current of the pulse generated by an OFC generator. As can be seen from the data given in Table 2, a twofold increase in magnetic projectile velocity doubles the signal amplitude. Power delivered in the load is proportional to the square of the projectile velocity. But, as the magnetic projectile velocity is increased, the duration of the generated pulse

decreases. Therefore, the energy delivered to the load is directly proportional to the velocity of the projectile.

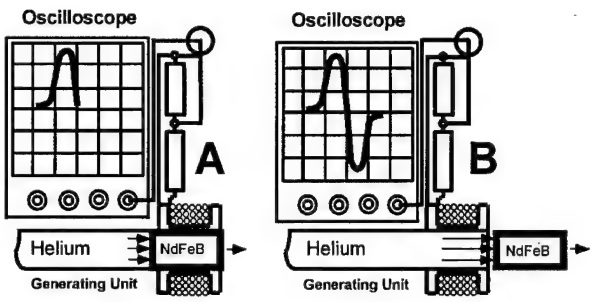

Figure 33. Schematic illustration of the operation of the OFC pulsed power generator.

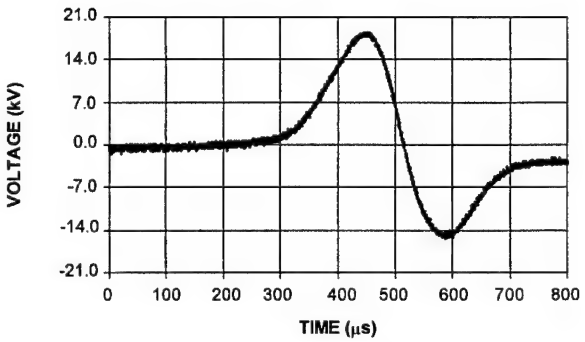

Figure 34. The OFC generator operated in the voltage mode.

Table 2. High-voltage pulse parameters as a function of the velocity of a magnetic projectile (NdFeB cylinder: D = 1.3 cm, L = 1.9 cm). R_{Load} = 55 kΩ.

Velocity (m/s)	Peak-to-Peak Voltage (kV)	Pulse Duration (μs)	Pulsed Power (kW)	Energy (J)
130	12.5	150	0.65	0.2
184	18.1	115	1.5	0.34
262	24.1	80	2.6	0.42
290	27.2	75	3.36	0.5

It should be noted that in the process of generating high-voltage pulses, some coils failed due to the electrical breakdown that took place between the coil turns which means, it is necessary to use a strong inter-layer insulation and take into account transient field distributions.

The calculation of the rate of variation of the magnetic flux in a coil, which is induced by NeFeB magnetic projectiles (D = 2.5 cm, L = 1.9 cm and D = 1.3 cm, L = 2.5 cm) gives a high operating efficiency for an open-magnetic-circuit-based generator. A pulse-generating element efficiently entraps over 60% of the magnetic flux produced by the NdFeB magnet in the closed ferromagnetic circuit.

We have performed a study of the pulse generation with magnetic projectiles having various dimensions to obtain information about the effect of the electromagnetic pulse generated across the coil. Experiments carried out with different length coils have shown that in the voltage mode the optimum (from the viewpoint of energy delivery at the load) length of the magnetic projectile is 1 to 1.5 times the length of the coil of the OFC generator.

The Current Mode

A typical waveform of the current pulses produced by an OFC generator operated in the current mode (low-resistance load) is shown in Fig. 35. The velocity of the 2.5 cm diameter and 2.5 cm length NdFeB projectile is 370 m/s. The peak-to-peak current released in a 7.2 mΩ load is 0.87 kA. A series of measurements have been carried out to investigate the effect of the

velocity of the magnetic projectile on the peak current of the pulse generated by an OFC generator. Experiments have shown that the current pulse amplitude is directly proportional to the velocity of the projectile. We carried out experiments with various shapes of the wire (rectangular wire, tape, round wire of different diameters), different number of layers, different lengths of the generating unit, and different loads. A great body of data obtained in the experiments has shown that there exists an optimum design for the generating unit, for the current mode of the OFC generator, which will be different for each application. In particular, for a coil with diameter 2.5 cm and length 1.9 cm, the optimum number of turns is eight for the current mode. The turns should be wound with 2.2 mm round copper wire in one layer. As experiments show, the optimum number of turns, type and diameter of wire depend primarily on the length and diameter of the ferromagnetic projectile and the resistance of the load.

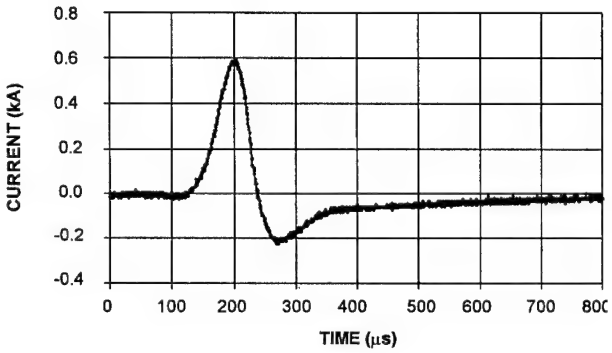

Figure 35. The OFC generator operated in the current mode (an NdFeB projectile).

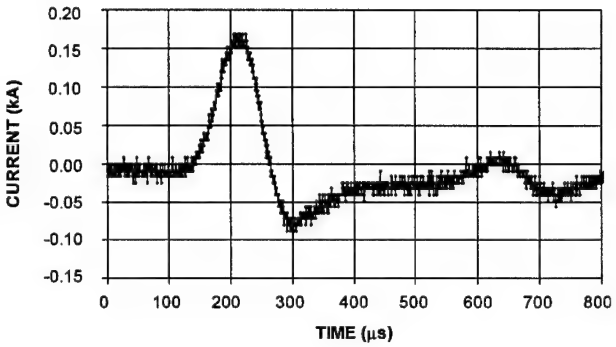

Figure 36. The OFC generator operated in the current mode (a $BaFe_2O_3$ projectile).

Figure 36 presents a typical waveform of the high current pulses produced by an OFC generator operated in the current mode with the 2.5 cm diameter and 2.5 cm length ceramic (Barium Strontium Ferrite) projectile moving with a speed of 310 m/s. The experiments have shown that the amplitude of the current pulses produced is a factor of 3 lower for the ceramic magnetic projectiles compared with NdFeB projectiles, which is in agreement with the residual magnetization ratio (2.8) for these materials.

It should be noted that the voltage mode and the current mode ensure the highest amplitude of the pulsed voltage and the pulsed current correspondingly, but does not provide the highest energy release at the load. Experiments have shown that for each size of the magnetic projectile there exists an optimal combination of the generating system design and the load resistance ensuring the most efficient release of pulsed energy at the load.

Simple calculations show that the energy released at the load of each generating module makes up no more than 0.4% of the kinetic energy of the NeFeB projectile. We have measured the speed of a ferromagnetic projectile before and after passage through ten generating modules with 2.7 J of energy released in each module. The experiment has shown that the reduction in the speed of a NdFeB projectile (D = 2.5 cm, L = 1.9 cm) is not over 1.5%. Thus, a ferromagnetic projectile accelerated to a high speed may provide efficient energy production in 50-100 generating modules.

The Charging and Integrating Modes

The operation of the OFC generator in the charging mode is illustrated in Fig. 37. In these modes, the loads of the generating modules are high-voltage capacitors. The electrical energy produced by the coils charges the capacitor banks. Figure 38 illustrates the waveforms of high voltage on capacitor banks which are charged by the energy produced in three generating modules.

Several generating modules connected in series provide multiplication of energy. This is the integrating mode of pulsed power generation. Figure 39 illustrates the operation of the OFC generator in the integrating mode. Experiments have shown that there are no losses in the integrating mode: the voltage and the energy stored by each capacitor bank is the sum of the total energy generated by the modules connected in series. Figure 40 gives a typical waveform of the voltage produced by the OFC generator in the integrating mode. The energy gain from each generating module is distinctly visible.

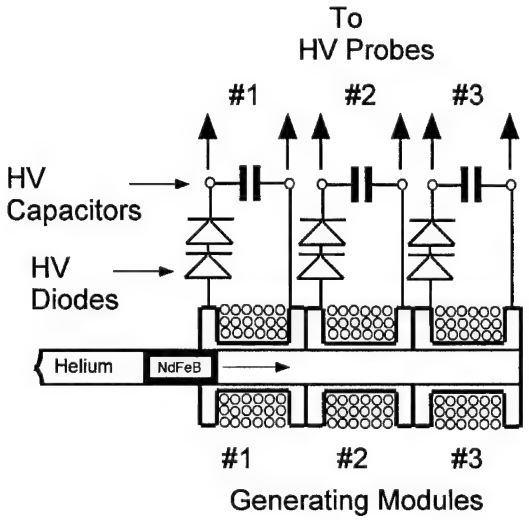

Figure 37. Schematic illustration of the operation of the OFC generator in the charging mode.

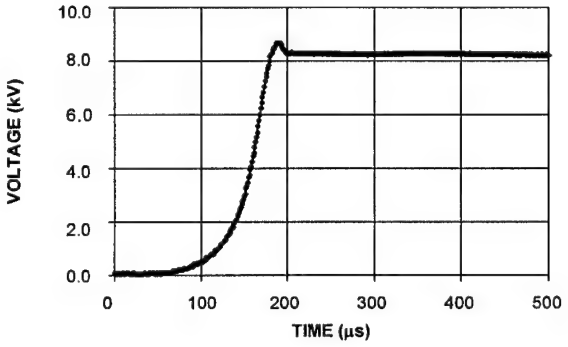

Figure 38. The waveforms of the voltage on capacitor banks which are charged by the energy produced in generating modules

A series of 30-50 generating modules would make it possible to produce a high energy pulse with a peak voltage of 300-500 kV with comparatively low velocities (500-900 m/s) and comparatively small dimensions (4-5 cm) of the magnetic projectile. A necessary component of such a circuit is a triggered high-voltage switch that would switch the pulsed energy into the load as the pulsed high voltage peaks.

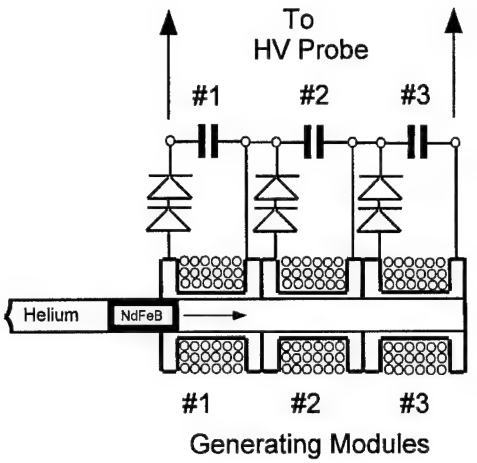

Figure 39. Schematic illustration of the operation of the OFC generator in the integrating mode.

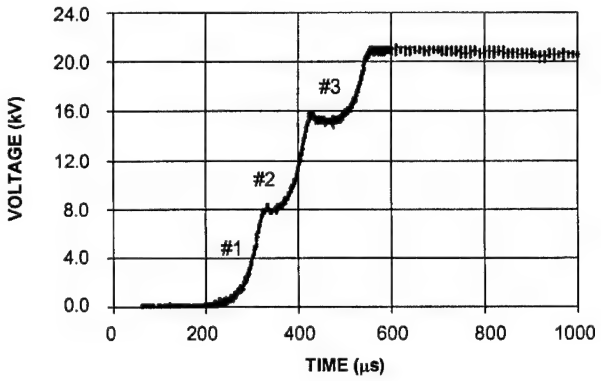

Figure 40. The OFC generator operated in the integrating mode. Amplitude of integrated signal 21.6 kV.

Closed Ferromagnetic Circuit Pulsed Power Generation

A schematic showing the operation of a pulse generator based on a closed ferromagnetic circuit is presented in Fig. 41. The key component in a CFC generator is a ferrite ring. The ferrite element of the CFC had an air gap of width of 2 mm which was made by cutting the ferrite ring in the center of the U-channel cut for projectile barrel (the U-channel diameter was made equal to the external diameter of the gas gun barrel).

The high-power pulsed electric signal was generated in the coil which was wound on the CFC ferrite element throughout its perimeter. The magnetic projectile moves with high velocity into the cylindrical attachment and then into the ferrite element of the CFC. The magnetic flux of the magnetic projectile closes through the CFC ferrite element, first partially and then (at the instant the projectile closes the air gap) almost completely. The variation in the magnetic flux inside the ferrite core generates the voltage in the coil wound on the core.

The experiments have shown that the amplitude, duration, waveform, and all other parameters of the electric pulse depend on many factors, the more important of which are as follows: (1) The magnetic characteristics of the projectile material. (2) The magnetic characteristics of the material of the CFC core: materials with low electric conductivity (to suppress the formation of eddy currents in the core), good frequency characteristics, etc. are required. (3) The geometrical proportions of the system. (4) The velocity of the projectile.

We have performed a study of the generation of multiple sinusoidal signals in CFC generators. The principle of the generation of a repetitive sinusoidal signal in a CFC generator is as follows. The magnetic projectile is a multicomponent system: magnetic disks alternating with dielectric nonferromagnetic interlayers. The multi-component magnetic projectile moves at a high speed into the cylindrical attachment and moves inside the CFC core. At the instance the air gap in the CFC core is closed or opened by the first magnetic disk, the process described in the previous Section occurs in the CFC core and in the inductance coil. This process results in the generation of a full-period wave. After the first magnetic disk, a short interval follows the second magnetic disk that also generates a full-period wave, and so on. The interval between two waves is determined by the thickness of the dielectric layer between the magnetic disks and by

the speed of the composite projectile. The number of periods is determined by the number of magnetic disks in the multicomponent magnetic projectile.

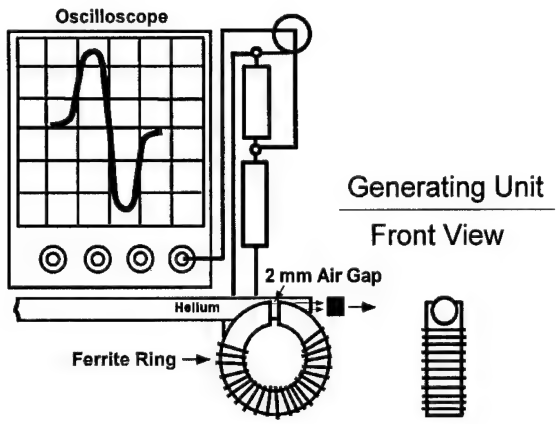

Figure 41. Schematic illustration of the operation of the closed ferromagnetic circuit pulsed generator.

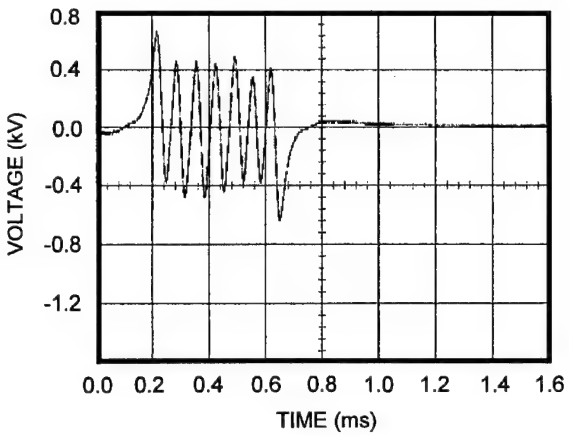

Figure 42. Multiple signal generated by the CFC generator.

A series of experiments have been performed to investigate the generation of multiple signals with different numbers of magnetic disks in the multicomponent magnetic projectile. An oscillogram obtained for a multicomponent projectile with seven ceramic disks (1.27 cm diameter and 0.5 cm length of each) is shown in Fig. 42 where seven sinusoids follow sequentially and have nearly the same amplitude. That is, the generated repetitive signal has a perfect waveform showing no breaks or distortions. The process of signal generation repeats without attenuation.

An analysis of the results of our study on the pulse generation in closed ferromagnetic circuits has shown that for the generation of a high-power periodic signal it would be preferable to harness the motion of a multicomponent projectile not along, but across the ferromagnetic toroid. A schematic of a CFC explosive generator intended to produce high-power microwave pulses is shown in Fig. 43. The core, made of a magnetically soft ferromagnetic material has an air gap whose diameter is equal to the diameter of the multicomponent magnetic projectile. A coil is wound on the core to produce a signal. The ferromagnetic disks constituting the multicomponent magnetic projectile are separated by nonmagnetic disks. The ferromagnetic disks are magnetized normal to the axis. With that, the N-S poles of the neighboring ferromagnetic disks are oriented oppositely. Prior to a shot, the ferromagnetic projectile is oriented in such a way that the direction of the N-S poles of the magnetic disks coincide precisely with the direction that will cause optimum magnetization of the magnetic core.

As the multicomponent magnetic projectile moves through the air gap of the core, the latter is magnetized by the magnetic disks alternately in two opposite directions. The variations in the magnetic flux have the result that high-frequency repetitive oscillations are generated in the coil. One multicomponent projectile could contain 300-1000 thin magnetic disks. When the projectile executes a complete cycle of motion through the magnetic core, 300-1000 periods of high voltage oscillations will be generated in the series connected generating modules. This high voltage signal can be used to generate high-power alternating pulses at the load.

Explosively Driven Moving Magnet Generators

The design of explosively driven generator using a moving magnetic projectile is shown in Fig. 44. Explosive experiments have shown that the best option for generators using a moving magnetic projectile is to utilize the energy of the gases formed as a result of explosive burning rather than the energy of the flyer plate accelerated under the action of explosive burning. The explosive of preference is not C-4, but a military propellant charge which shows a high burning velocity and a high energy of the explosive gases. At the same time, its action is nondestructive for the explosion chamber of the generator. This is of critical importance because the integrity of the explosion chamber makes it possible to utilize the whole energy of the explosive gases for acceleration of the ferromagnetic projectile. For a more uniform detonation and a more efficient release of explosive gases we used a type EWB-1001 small-diameter detonator (while in the previous experiments we used an RP-501 detonator). The spherical aluminum flyer plate works like the burst diaphragm in this device.

To protect the explosion chamber, we used an all-metal stainless-steel bowl. In all experiments, NdFeB cylinders (D = 2.5 cm, L = 1.9 cm) were used as ferromagnetic projectiles. The magnetic projectiles were dressed in lexan streamlined cartridges. The generator included seven identical pulse-generating coils. These coils, for the case of low resistance load (the Current Mode), were developed based on the data obtained in experiments with a gas gun. All coils were loaded by 5 mΩ, low-inductance loads. The signal was picked from the middle point of the load (2.5 mΩ). Calibrated Rogowski coils with integrators were used to measure the current flowing in the load circuit.

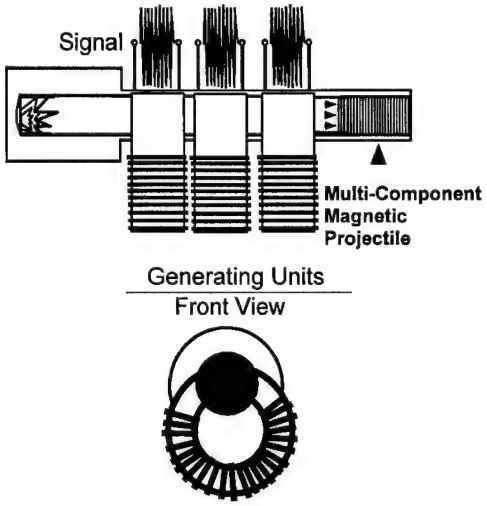

Figure 43. Schematic of explosively driven closed ferromagnetic circuit microwave generator.

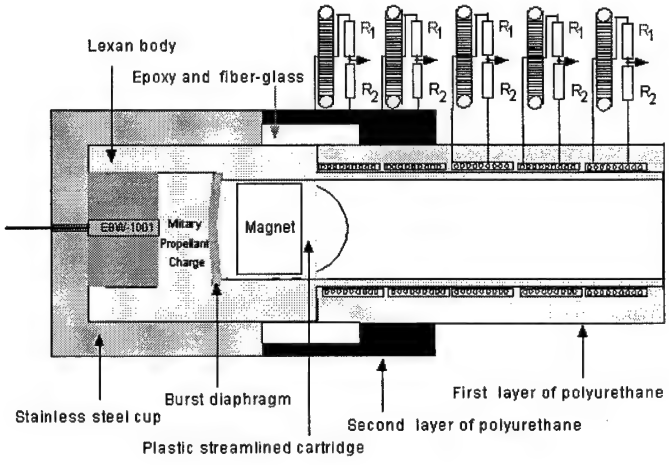

Figure 44. Schematic of explosively driven open ferromagnetic circuit pulse generator.

The general appearance of an explosively driven moving magnet generator in the charged state is presented in Fig. 45. Figure 46 shows two pictures taken in the process of explosive operation. The destruction of the generator body near the metallic bowl is distinctly visible. The generator after the test is shown in Fig. 47.

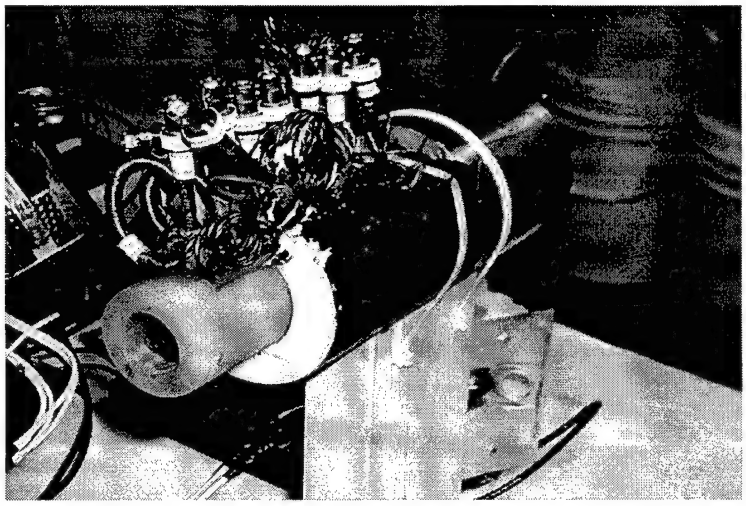

Figure 45. Explosively driven moving magnet generator in the charged state. The ferromagnetic projectile is an Nd35 cylinder D = 2.5 cm, L = 1.9 cm. The load resistance is 5 mΩ. Explosive (military propellant charge) charge mass is 15 g.

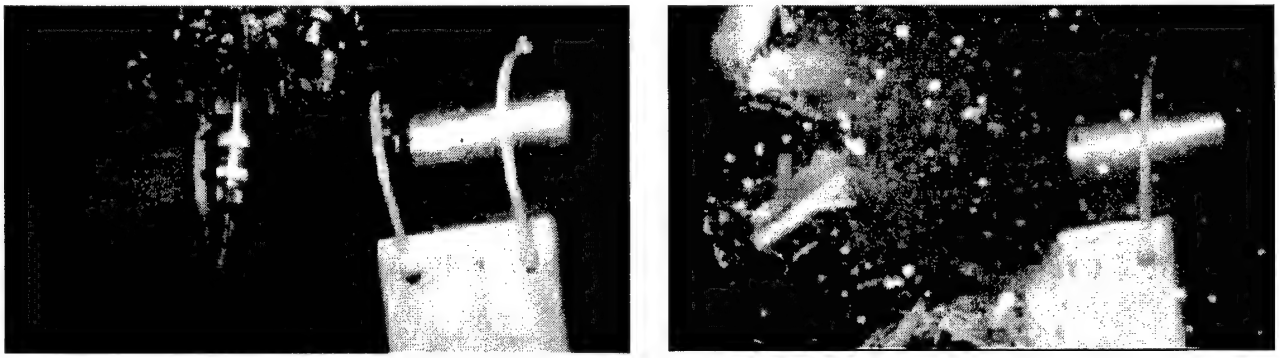

(a) (b)

Figure 46. Explosive operation of the moving magnet generator. The picture (a) was taken at the moment of detonator ignition. Shot-to-shot interval is 1 ms.

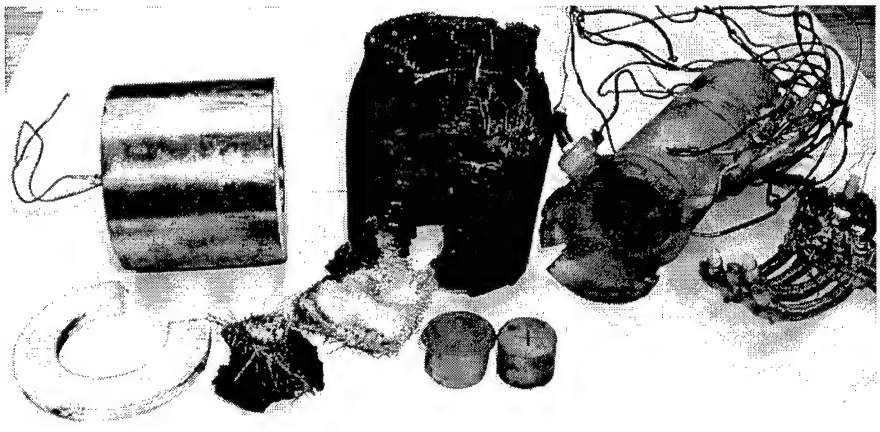

Figure 47. Explosively driven moving magnet generator after the test.

Figures 48 gives current oscillograms (RC signals) taken from Generating Coils # 4 and 5. All current waveforms have a shape close to sinusoidal. Each oscillogram has half-waves of opposite polarity appearing as the ferromagnetic projectile comes into and out of the generating coil. Noteworthy is the similarity of the oscillograms obtained in the explosive test and in the test with a gas gun (Figs. 35-36).

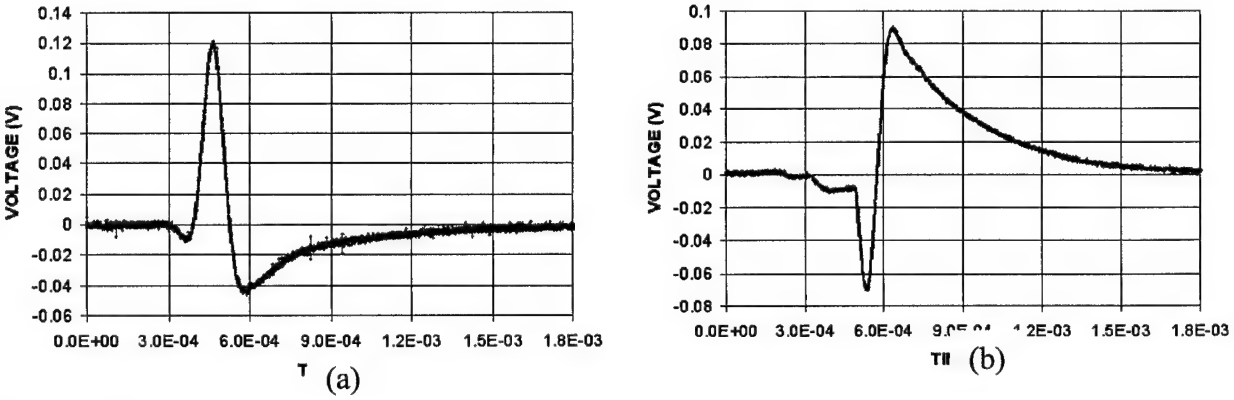

Figure 48. Explosive operation of the moving magnet generator. The ferromagnetic projectile is an Nd35 cylinder D = 2.5 cm, L = 1.9 cm. Waveform of the current pulse (signal from a Rogowski coil). (a) - Pulse-Generating Coil #4 (5 A/mV). (b) - Pulse-Generating Coil #5 (4.9 A/mV).

The maximum signal is observed for the fourth generating coil. The current peak-to-peak amplitude is about 0.9 kA. The signals from the third, fifth and sixth generating coils are smaller. The peak-to-peak amplitude of the signals from the third and fifth coils is 0.6 kA and 0.8 kA, respectively. The projectile had less velocity in the third coil in comparison with the fourth coil. In the fifth and the sixth coils, obviously the velocity decreased due to the detachment of the generator body, the exhaust of explosive gases, and the deceleration of the ferromagnetic projectile in the generator barrel.

Summary

The experiments performed with a gas gun kinetic energy converter have shown that even with comparatively low velocities of the magnetic projectile (200-350 m/s) and small dimensions of the pulse generating system, the peak voltage of the pulses produced by the OFC generator reaches several tens of kilovolts, peak current reaches kiloamperes and the energy delivered at the load is a few Joules. The devices show high capabilities for producing electric pulses. The operation efficiency is comparable to generators using ferroelectric media and compact flux compressor generators using the field of permanent magnets.

Generating modules connected in series for the charging mode will make it possible to produce a high energy pulse with a peak voltage of 300-500 kV. The experimentally obtained data show that the relation between the high voltage pulse duration and amplitude is linear to a rather high accuracy with the velocity of the magnetic projectile. With explosively driven magnetic projectiles we expect peak currents of kilo-amperes and the energy to be in the tens of Joule range.

It has been shown experimentally that a CFC generator is capable of generating not only single high voltage pulses, but also repetitive oscillations. The amplitude, repetition period, and number of the repetitive oscillations are determined by the material of the multicomponent magnetic projectile, by its speed, by the number of magnetic disks in the multicomponent projectile, by the properties of the ferrite ring, and by the geometrical dimensions of the system. Special design, proper choice of ferromagnetic materials, explosively driven multicomponent ferromagnetic projectiles and using resonance circuits can make it possible for CFC generators to attain the capability of producing pulsed microwave power.

The experiments performed have demonstrated the possibility of producing a series of high-current pulses by explosively driven generators using ferromagnetic projectiles. The results obtained show that it is it is necessary to improve the protection of the generator body near the explosive chamber. This will be done in the next series of explosive tests. Further investigations are needed with the objectives to study the acceleration of a magnetic projectile under the action of explosives and to improve the parameters of the pulses produced by this type of generator. Particular attention should be given to the simulation of the moving magnet generation by the Maxwell 3D code (Eddy Current Solver), the Maxwell 2D (Transient Solver) and by the PSpice code (simulation of equivalent circuits).

IV. HIGH CURRENT, HIGH VOLTAGE PULSED TESTING OF RESISTORS

Experimental

For the purpose of high current, high voltage pulsed testing of resistors, a setup has been designed that includes high voltage pulse generators, a switching unit, a box for the components to be tested, and a system for pulse signal detection. Figure 49 shows a layout of the setup. High voltage probes (Tektronix P6015), wideband current transformers (Pearson Electronics, Inc., model 110A), and current dividers were used for pulsed voltage and current measurements. The testing of resistors was performed in two modes: pulsed high voltage mode and pulsed high current mode.

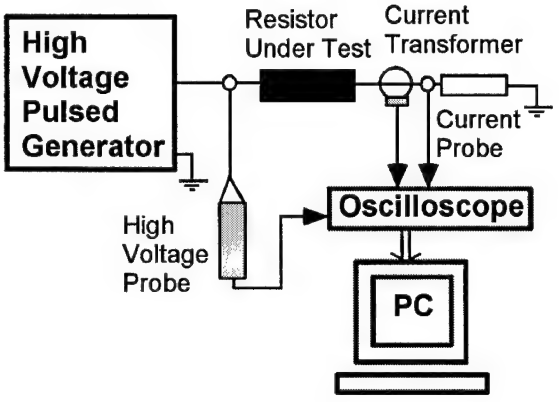

Figure 49. Schematic diagram of a setup for pulsed, high energy testing of resistors.

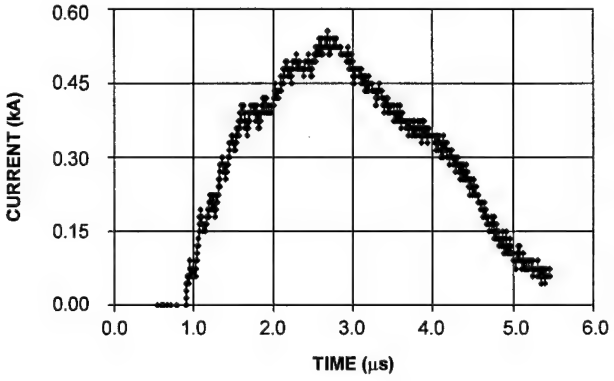

Figure 50. Waveform of the pulsed threshold current passed through an Allen Bradley 27 Ω/0.5 W carbon composition resistor.

High Current Pulsed Testing

In the pulsed current mode, the critical modes of pulsed heating of resistors were determined under the effect of current flow. Two types of pulsed voltage generators were used: a cable generator (the pulse durations were 100, 250, 700 and 1200 ns) and a spark-gap generator (pulse durations were 0.7, 2.4, 4.2, 8.5, 13 and 21 μs). The maximum voltage amplitude was 12 kV. The peak current was 3 kA.

Figure 50 presents a waveform of the current pulse which destroyed a carbon composition resistor manufactured by Allen Bradley of 0.5 W power rating. The shape of the current pulse follows without any distortion the shape of the voltage pulse. A carbon composition resistor before and after passing a high pulsed current is shown in Fig. 51.

Three different types of resistors have been tested in detail to determine maximum usable power at pulsed high voltage and pulsed high current: metal film, carbon film and carbon composition resistors of four different rated powers (0.25 W, 0.5 W, 1 W, 2 W).

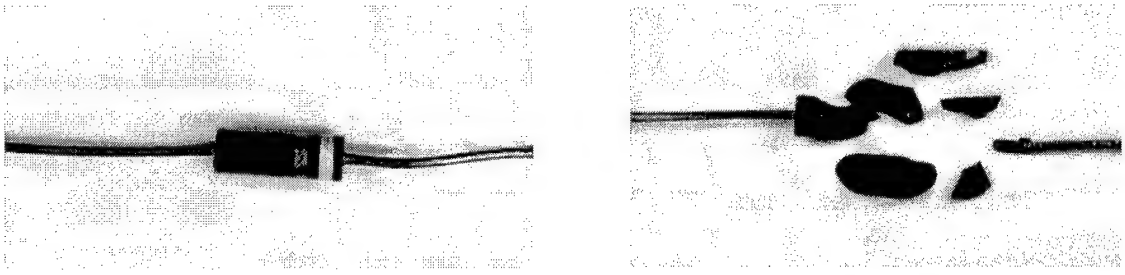

(a) (b)

Figure 51. Carbon composition resistor before (a) and after (b) passing a high pulsed current (see Fig. 49).

Our experiments have shown that the threshold pulsed power (P_F) that causes failure of the resistors depends on the duration and amplitude of the current pulse and on the power rating of the resistors. For each type of resistors and for each power rating the data were obtained on threshold pulsed energy, threshold pulsed power and integral of action in a wide range of pulse durations. Figure 52 shows the threshold pulsed power P_F for the carbon composition resistors plotted against the current pulse duration. Figure 53 shows the pulsed energy required to destroy the carbon composition resistors with various power ratings.

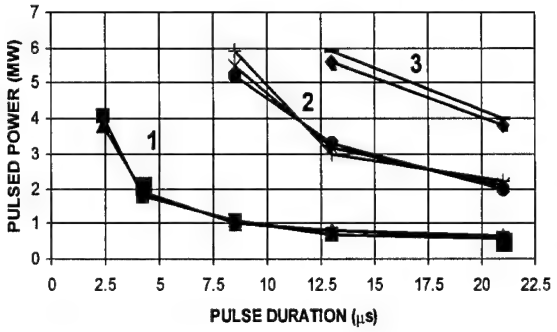

Figure 52. Threshold pulsed power P_F versus current pulse duration for 27 Ω carbon composition resistors 0.5 W (1), 1 W (2) and 2 W (3).

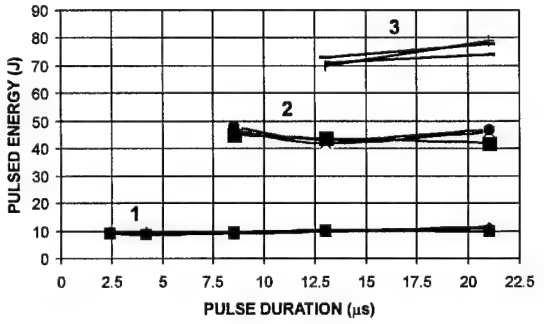

Figure 53. Pulsed energy destroying 27 Ω carbon composition resistors with power ratings of 0.5 W (1), 1 W (2) and 2 W (3).

Table 3 represents typical threshold characteristics versus pulse duration for carbon composition resistors of power ratings 0.5 W.

Table 3. Characteristics of the threshold pulse action for the carbon composition resistors 27 Ω/0.5 W.

Pulse duration (μs)	Current (A)	Voltage (kV)	Power (kW)	Energy (J)	Action integral (A^2 s)
2.4	400	10	4000	9.2	0.38
4.2	270	7.0	1890	8.5	0.031
8.5	200	5.4	1080	9.2	0.034
13	180	4.2	756	9.8	0.42
21	150	3.7	555	11.6	0.47

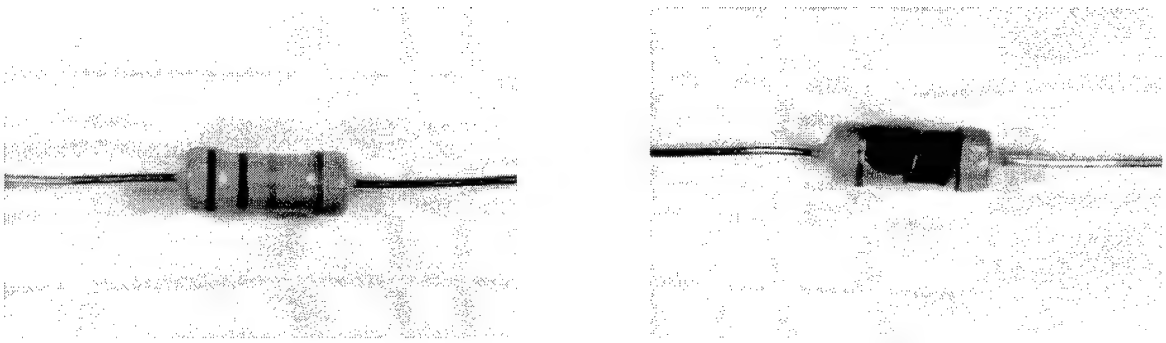

(a) (b)

Figure 54. A carbon film resistor 27 Ω/1 W before (a) and after (b) application of a high current pulse. The resistance of the resistor was 5 kΩ after high current pulsed action.

Figure 54 shows a carbon film resistor made by Xicon before and after passing a high pulsed current. High current action is accompanied by explosive removal of the protective paint coating. Table 4 represents typical threshold characteristics versus pulse duration for carbon film resistors of power ratings 0.5 W.

Table 4. Characteristics of the threshold pulse action for the carbon film resistors 27 Ω/0.5 W.

Pulse duration (μs)	Current (A)	Voltage (kV)	Power (kW)	Energy (J)	Action integral (A^2 s)
0.7	400	5.0	2000	1.4	0.11
1.0	300	4.9	1470	1.47	0.09
2.4	220	4.0	880	2.11	0.11
4.2	150	3.4	510	2.14	0.095
8.5	110	2.2	242	2.06	0.1

Figure 55 shows a metal film resistor made by RCA (Thompson Electronics) before and after pulsed action. Passing a high pulsed current is accompanied by explosive removal of the protective paint coating. Table 5 represents typical threshold characteristics versus pulse duration for metal film resistors of power ratings 0.5 W.

Table 5. Characteristics of the threshold pulse action for the metal film resistors 27 Ω/0.5 W.

Pulse dur. (μs)	Current (A)	Voltage (kV)	Power (kW)	Energy (J)	Action integral (A^2 s)
0.7	230	3.9	897	0.63	0.037
2.4	85	2.2	176	0.42	0.017
4.2	70	1.8	126	0.52	0.021
8.5	50	1.2	60	0.51	0.021

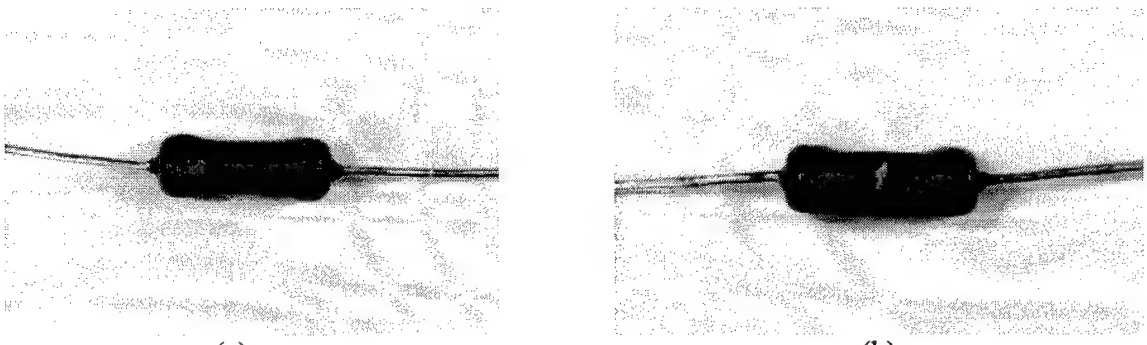

(a) (b)

Figure 55. An 27 Ω/1 W metal film resistor before (a) and after (b) application of a 0.7 μs/370 A current pulse. The resistance of the resistor was 4 MΩ after the pulsed action.

Summary

Analysis of the experimental data obtained in the study of the pulsed current action on carbon composition, carbon film, and metal film resistors leads to the following conclusions:

(1) Most stable to the action of a pulsed current are carbon composition resistors. Metal film resistors are most sensitive to pulsed currents. They withstand a pulsed loading by a factor of several tens less than carbon composition resistors and a factor of 2 or 3 lower than carbon film resistors.

(2) The threshold pulsed power withstood by carbon composition resistors within the range of pulse durations 2.4 - 21 μs is more than 10^6 times greater than their dc power rating and equals 1-5 MW.

(3) The power threshold and the processes occurring in resistors under high power pulsed action are apparently determined by the production technology and the materials used by the manufacturer.

(4) The experimental data on the limiting peak pulsed current and voltage, the action integral, and the threshold pulsed power and energy allow one to determine the threshold characteristics of the resistors over a wide range of pulse durations.

The data obtained in testing the resistors in the high pulsed voltage mode (with an electric field gradient of 30-70 V/cm) leads to the conclusion that carbon film resistors are most stable to the action of a high pulsed voltage. The carbon composition resistors of power rating 1 W are most sensitive to high pulsed voltages.

The experimental investigation of the threshold loading of the resistors in the high current mode and in the high pulsed voltage mode has shown that the mechanisms for the destruction of resistors have specific features for each mode. To gain an understanding of the mechanism for the destruction of resistors, the investigations are being continued.

V. HIGH ENERGY TESTING OF CAPACITORS

For the purpose of testing capacitors, a setup has been designed that includes a high voltage power supply, a switching unit, metallic tank for the components to be tested, and a system for signal detection. Figure 56 shows a layout of the setup. High voltage probes (Tektronix P6015 and Pintek HVP-40), wideband current transformers (Pearson Electronics, Inc., model 110A and Tektronix P6021), and current dividers were used for voltage and current measurements. Figure 57 shows the waveform of the voltage which destroyed 0.6 kV ceramic capacitor under the test.

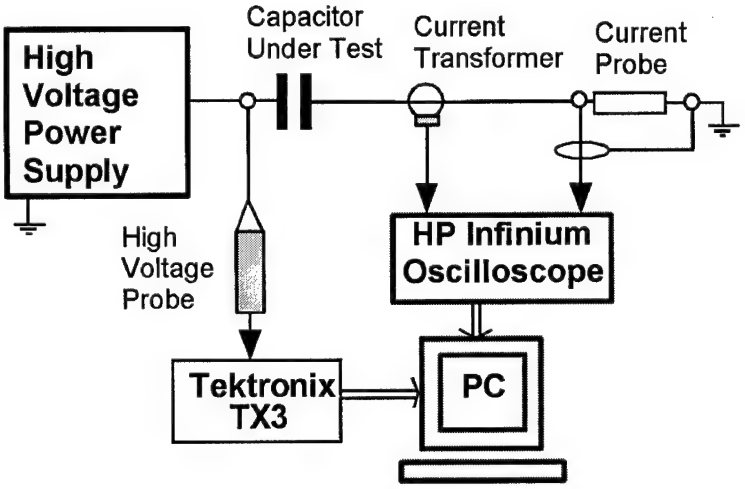

Figure 56. Schematic diagram of a setup for testing capacitors.

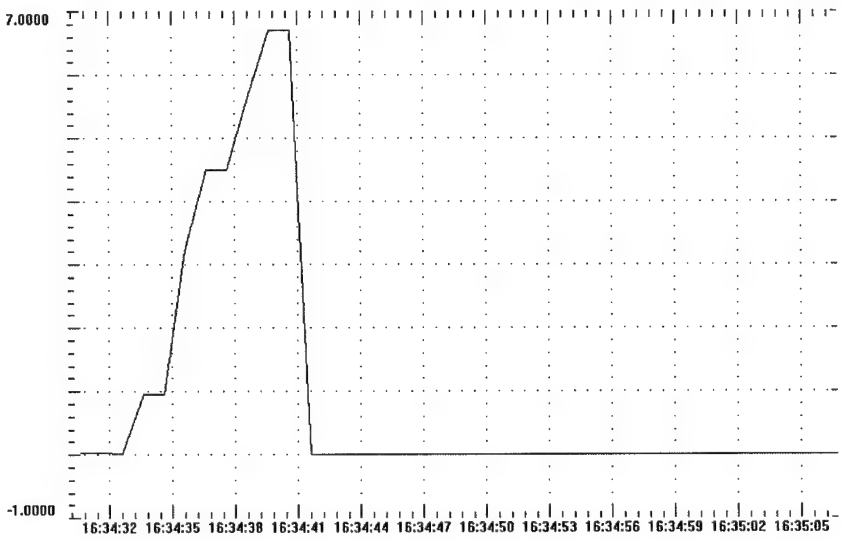

Figure 57. Waveform of the voltage across a 0.6 kV ceramic capacitor. Resistance of the capacitor before the test was more than 30 MOhm. Resistance of the capacitor after the test was 0.2 Ohm. Vertical axis is voltage. One big division equals one kV. Horizontal axis is time. One big division equals three seconds.

Testing of 0.6 kV ceramic capacitors in the second time range have shown that breakdown voltage is 7-8 kV, more than ten times higher than nominal voltage of the capacitors. Figure 58 through 60 shows a typical signal from the current probe for a 0.6 kV ceramic capacitor test. There are two current spikes before the main breakdown.

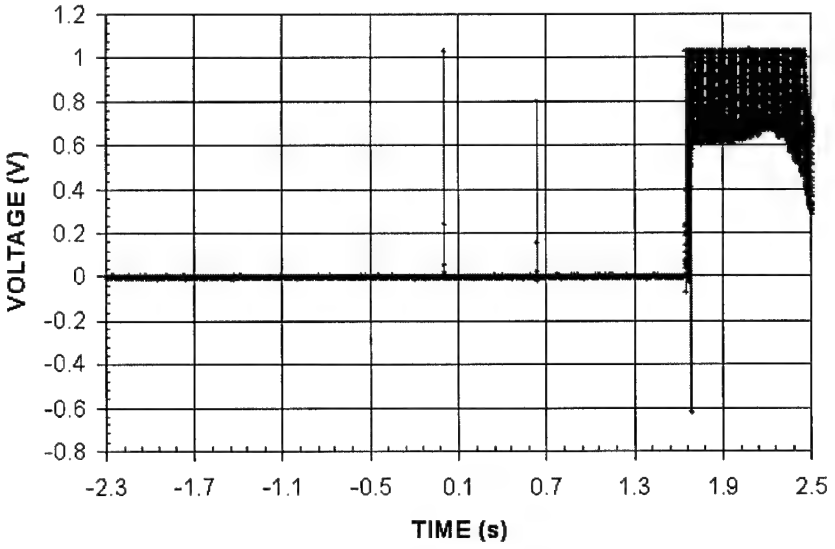

Figure 58. Signal from the current probe with a 0.6 kV ceramic test capacitor. Breakdown voltage 7 kV (Fig. 57).

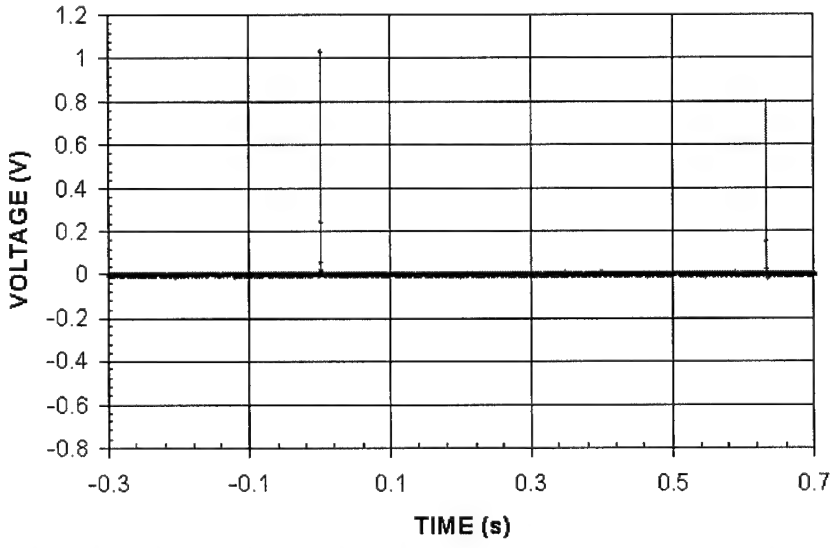

Figure 59. Signal from the current probe (Fig. 57) with a magnified time scale. There are two distinctly visible prebreakdown current spikes.

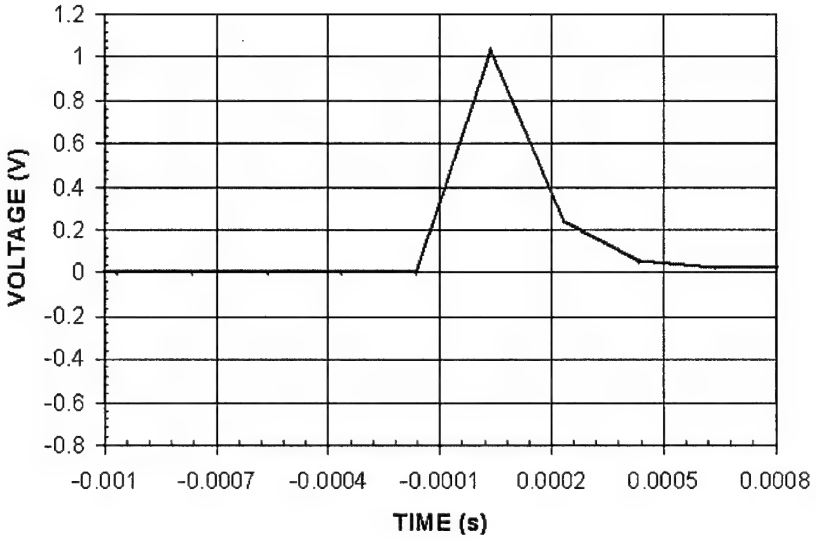

Figure 60. First current spike in a magnified time scale.

The experimental investigation of the threshold loading of the capacitors has shown that the mechanisms for the destruction of capacitors have specific features. We carried out a series of tests with ceramic and thin film capacitors having nominal voltages, 0.6 - 3 kV. The breakdown voltage ranged from 8 to 14 times higher than the nominal voltage of the capacitors. There were no visible changes in the capacitors' protective paint coating. The only change was a significant reduction of the resistance of the capacitors after tests. To gain an understanding of the mechanism for the breakdown of capacitors, the investigations are being continued. We plan to systematically test ceramic, tantalum, polypropylene capacitors having nominal voltages of 0.5 - 5 kV in both a five second mode as well as a microsecond mode.

VI. CHEMICAL GETTERING AT HIGH PRESSURES

Electron beam driven high power microwave systems require high vacuum but, at the present time, this implies active pumping due to outgassing from the non-bakeable system components. It is desirable to be able to use inexpensive materials (such as Lexan) but yet avoid having to use a continuous vacuum pumping system. We have made a small effort to determine if it is possible to use chemical techniques to pump down a system with such non-bakeable materials after it has been initially pumped down and then allowed to outgas back to pressures of maybe a few Torr. This chemical gettering technique is different from conventional electronic vacuum tube gettering techniques by the pressures at which it is expected to operate. The initial results are promising and were presented at the 1998 IEEE International Conference on Plasma Science, Raleigh, NC, June 1998.

The experiments on evacuating a closed vessel by use of a chemical reaction to getter the ambient gas have now been concluded. The results show that it is possible to choose a chemical reaction, which will reduce the gas pressure dramatically. For example, sodium hydroxide was used to reduce the pressure of carbon dioxide (a common residual gas in vacuum vessels) from 800 mTorr to less than 100 mTorr in 100 seconds. The chamber volume was 2×10^{-2} m^3 and the experiment was repeated 16 times before the NaOH was exhausted. A journal paper on these experiments has been accepted by the Journal of Vacuum Science and Technology.

The investigator in charge of this work has moved to Mercer University (Dept. Chairman).

SUMMARY OF COLLABORATIVE ACTIVITIES

1. M. Kristiansen attended a classified meeting on compact HPM radiation devices at Los Alamos National Laboratory in April 1998.

2. M. Kristiansen attended a classified meeting on compact HPM radiation devices in Huntsville, Al in June 1998.

3. Dr. M. Kristiansen met with Mr. F. MacDougall and Joel Ennis of Maxwell/ Physics International Co. in San Diego on July 24, 1998 to discuss performance limits on energy storage capacitors and to lay the ground for future cooperation.

4. M. Kristiansen, J. Dickens and S. Shkuratov attended the IEEE International Pulsed Power Conference in Monterey, CA on June 27-30, 1999 and presented two papers.

5. TTU hosted Drs. A. Prischipenko and V. Onoochin on July 2, 1999 for a seminar on RF munitions. Representatives attended this seminar from LANL, CIA, and White Sands Missile Range.

6. A cooperative program (supported by the US Army Strategic Defense Command) was established with a small business (Applied Physical Electronics, Austin, TX) to attempt to drive a BWO with a very compact Marx generator system.

7. M. Kristiansen and J. Dickens attended the classified 9th High Power Microwave and Radio Frequency Conference at Kirtland Air Force Base, Albuquerque, NM on May 11-13, 1999.

8. M. Kristiansen, J. Dickens and S. Shkuratov attended the IEEE International Conference on Plasma Science in New Orleans, LA on June 4-7, 2000 and presented two papers.

Synergism's with Other Research Programs

This NWV program is closely related to TTU's new MURI/AFOSR program on Explosive-Driven Pulsed Power Generation since both depend on explosive technology. The NWV devices may also form the basis for the required seed sources for the MURI devices.

Dr. Larry Altgilbers of the US Army Space and Missile Defense Command in Huntsville, AL was kept continually updated on our research progress and received copies of all our reports and papers. Dr. Altgilbers also visited our laboratory.

Several classified programs also can benefit from the information gained here and have shown interest in our work but direct cooperation with these programs is not feasible under the restriction of a 6.1 basic research program.

SUMMARY OF PUBLISHING ACTIVITIES

Journal Papers

1. "A Review of Short Pulse Generator Technology", J. Mankowski and M. Kristiansen, *IEEE Transactions on Plasma Science,* Vol. 28, No. 1, pp. 102-108, 2000.

2. "Pulse Generation Using Open and Closed Ferromagnetic Circuits", S.I. Shkuratov, M. Kristiansen, J. Dickens, L.L. Hatfield, and R. Martin, accepted for publication in *IEEE Transactions on Plasma Science.*

3. "High Current and High Voltage Pulsed Testing of Resistors", S.I. Shkuratov, M. Kristiansen, J. Dickens, L.L. Hatfield, and E. Horrocks, accepted for publication in *IEEE Transactions on Plasma Science.*

Conference Papers

1. "Chemical Gettering at High Pressures", R.D. Peters, L.L. Hatfield and M. Kristiansen, IEEE International Conference on Plasma Science, Raleigh, NC, June 1998.

2. "Pulsed Electrical System", M. Kristiansen, ElectroMed 99, Norfolk, VA, April 1999 (Invited Paper).

3. "Pulsed Power Generation Using Ferromagnetic Circuits", S.I. Shkuratov, M. Kristiansen, J. Dickens, L.L. Hatfield, and R. Martin, Proceedings of 12th International Pulsed Power Conference, Monterey, CA, June 1999, Vol. II, pp. 716-719.

4. "High Energy, Pulsed Testing of Resistors", S.I. Shkuratov, M. Kristiansen, J. Dickens, L.L. Hatfield, and E. Horrocks, Proceedings of 12th International Pulsed Power Conference, Monterey, CA, June 1999, Vol.II, pp. 712-715.

5. "Pulsed Generators Based on Shock Demagnetization of Hard Ferromagnetic Materials", S.I. Shkuratov, M. Kristiansen, and J. Dickens, Proceedings of the 27th International Conference on Plasma Science, New Orleans, LA, June 2000, p. 277.

APPENDIX

The following appendix lists the abstracts for all journal and conference papers and also lists the recently submitted journal abstracts.

IEEE Transactions on Plasma Science. Vol. 28, No. 1, pp. 102-108, 2000.

ABSTRACT #1

A REVIEW OF SHORT PULSE GENERATOR TECHNOLOGY

John Mankowski and Magne Kristiansen
Texas Tech University
Pulsed Power Laboratory
Departments of Electrical Engineering and Physics
Lubbock, TX 79409-1051

Today's ultra-fast, pulsed generators are capable of producing high voltage pulses (> 1 kV) with fast, leading-edge risetimes (< 1 ns). A review of generator implementation methods is presented that includes a detailed discussion of the various circuit designs and primary switch types. A list of commercially available high voltage pulse generators is provided. All these generators are capable of risetimes less than a few ns and voltage greater than several hundred kilovolts. Finally a brief description of the primary switch types, reed, sparkgap, and solid state is presented.

IEEE Transactions on Plasma Science. In print.

ABSTRACT #2

HIGH CURRENT AND HIGH VOLTAGE PULSED TESTING OF RESISTORS

S.I. Shkuratov, *Member, IEEE*, M. Kristiansen, *Life Fellow, IEEE*, J. Dickens, *Member, IEEE*, L.L. Hatfield, *Member, IEEE,* and E. Horrocks

Abstract— Three types of resistors have been tested to determine maximum usable power at pulsed high voltage and pulsed high current. Experiments were carried out using high voltage cable generators, spark-gap generators and thyratron drivers. Pulse durations were varied from 0.7 μs to 21 μs. The pulse amplitudes were varied from 1 kV to 35 kV. The peak current reached was 3 kA. Metal film, carbon film and carbon composition resistors of four different rated powers (0.25 W, 0.5 W, 1 W, 2 W) have been tested. Data are given for the limiting pulsed power and energy for each type of resistor in nanosecond and microsecond time ranges. The experimental investigation of the threshold loading of the resistors in the high current pulsed mode and in the high voltage pulsed mode has shown that the process of destruction of resistors has specific features for each mode. The mechanisms of failure and destruction of resistors under the action of high voltage and high current pulses are discussed.

IEEE Transactions on Plasma Science. In print.

ABSTRACT #3

PULSE GENERATION USING OPEN AND CLOSED FEROMAGNETIC CIRCUITS

S.I. Shkuratov, *Member, IEEE*, M. Kristiansen, *Life Fellow, IEEE*, J. Dickens, *Member, IEEE*, L.L. Hatfield, *Member, IEEE,* and R. Martin

Abstract—Results are presented of an experimental study of the generation of high-voltage and high-current pulses in generators designed as open and closed ferromagnetic circuits. Experiments were carried out using a light gas gun system. The magnetic projectiles were composed of ferromagnetic disks having 1.27 and 2.54-cm diameters. It has been shown that with velocities of the magnetic projectiles of 200-380 m/s, the peak voltage of the pulses produced by the generators reach several tens of kilovolts, peak current reaches kiloampere and the energy delivered at the load is a few Joules. Generating modules connected in series will make it possible to produce a high energy pulse with a peak voltage of a few hundred kV. It has been shown that a closed ferromagnetic circuit generator is capable of generating not only single high voltage pulses, but also repetitive oscillations. Data are given for the effects on the amplitude of high voltage pulses caused by the length and velocity of the ferromagnetic projectiles and the design of the generating unit for both high voltage and high current modes of pulsed power generation.

Proceedings of IEEE International Conference on Plasma Science, Raleigh, NC, June 1998.

ABSTRACT #4

CHEMICAL GETTERING AT HIGH PRESSURES

R.D. Peters*, L.L. Hatfield, and M. Kristiansen
Departments of Electrical Engineering and Physics
Texas Tech University, Lubbock, TX 79409-1051

Through experiments in which carbon dioxide was allowed to react with a mixture of sodium hydroxide and perchlorate in a closed container, it has been demonstrated that sealed vessel can experience significant pressure reduction during a chemical reaction that is unconventional, as compared to a common vacuum techniques.

* Present Address: Department of Physics, Mercer University

ElectroMed99,Norfolk, VA, April 12-14, 1999 (Invited Paper).

ABSTRACT #5

PULSED ELECTRICAL POWER SYSTEMS

M. Kristiansen
Texas Tech University
Pulsed Power Laboratory
Departments of Electrical Engineering and Physics
Lubbock, TX 79409-1051

The basic pulsed power concepts and the most common pulsed power circuits are review briefly. Several novel, short pulse devices are described in some more detail. Most of these devices are developed in Russia and now commercially available through various US representatives. These devices can produce output voltage exceeding 100 kV (1 MV for single pulse) into 50 Ohm load with pulse widths as short as 150 ps and repetition rates of several thousand pulses per second. They are compact and reliable and several of them have been used extensively for various research projects in our laboratory.

This work was supported primarily by New World Vista Program in AFOSR.

Proceedings of 12th International Pulsed Power Conference, Monterey, California, June 27-30, 1999.

ABSTRACT #6

PULSED POWER GENERATION USING FERROMAGNETIC CIRCUITS

S.I. Shkuratov, M. Kristiansen, J. Dickens, L.L. Hatfield, and R. Martin
Pulsed Power Laboratory, Departments of Electrical Engineering and Physics
Texas Tech University, Lubbock, TX 79409-3102

Results are presented of investigations of the generation of high voltage pulses in generators designed as open and closed ferromagnetic circuits. Experiments were carried out using a light gas gun system. The magnetic projectiles were composed of NdFeB discs having 1.27 and 2.54-cm diameters. Data are given for the effects on the amplitude of high voltage pulses by the length and velocity of the ferromagnetic projectiles and the design of the generating unit for both high voltage and high current modes of pulsed power generation. A detailed analysis is presented on the specific features of pulse power generators using open and closed ferromagnetic circuits. Fundamental limitations due to the physical processes occurring in systems like these are determined.

This work was solely funded by the New World Vistas Program in the Air Force Office of Scientific Research (AFOSR).

Proceedings of 12th International Pulsed Power Conference, Monterey, California, June 27-30, 1999.

ABSTRACT #7

PULSED, HIGH ENERGY TESTING OF RESISTORS

S.I. Shkuratov, M. Kristiansen, J. Dickens, L.L. Hatfield, and E. Horrocks
Pulsed Power Laboratory, Departments of Electrical Engineering and Physics
Texas Tech University, Lubbock, TX 79409-3102

Different type of resistors have been tested to determine maximum usable power at pulsed high current. Experiments were carried out using high voltage cable generators and spark-gap generators. Pulse durations were varied from 0.7 μs to 21 μs. The pulse amplitudes were varied from 1 kV to 12 kV. The peak current reached was 3 kA. Metal film, carbon film and carbon composition resistors of four different rated powers (0.25 W, 0.5 W, 1 W, 2 W) have been tested. Data are given for the limiting pulsed energy for each type of resistor in nanosecond and micro-second time ranges. The mechanisms of failure and destruction of resistors under the action of high voltage and high current pulses are discussed.

This work was solely funded by the New World Vistas Program in the Air Force Office of Scientific Research (AFOSR).

Proceedings of the 27th International Conference on Plasma Science, New Orleans, LA, June 4-7, 2000.

ABSTRACT #8

PULSED GENERATOR BASED ON SHOCK DEMAGNETIZATION OF FERROMAGNETIC MATERIAL

S.I. Shkuratov, M. Kristiansen, and J. Dickens

Departments of Electrical Engineering and Physics, Pulsed Power Laboratory,

Texas Tech University, Lubbock, TX 79409-3102

The design of an explosive-to-electric transducer that uses the remnant magnetization in ferromagnetic cylinders is presented. 10-25 g charge of high explosives was used. The active element was NdFeB cylinders with diameter 2.5 cm and length 1.9 cm. The current generated in the low-resistance load of the generator yielded a peak 0.4 kA. Results of simulation of an explosive-to-electric transducer by Maxwell 3D code is presented. A detail analysis is given on the specific features of pulse generation in a system like this.

This work was solely funded by New World Vista Program in the Air Force Office of Scientific Research (AFOSR).